

1 **Secondary formation dominated low molecular weight amines origins**
2 **in aerosols over the marginal seas of China**

3 Xiao-Ying Yang^{1,2}, Fang Cao^{1,2}, Chang-Liu Wu^{1,2}, Yu-Xian Zhang^{1,2}, Wen-Huai
4 Song^{1,2}, Yu-Chi Lin^{1,2}, Yan-Lin Zhang^{1,2*}

5 ¹. School of Ecology and Applied Meteorology and Atmospheric Environment Center,
6 Joint Laboratory for International Cooperation on Climate and Environmental Change,
7 Ministry of Education, Nanjing University of Information Science & Technology,
8 Nanjing 210044, China.

9 ². Jiangsu Key Laboratory of Atmospheric Environment Monitoring and Pollution
10 Control, Collaborative Innovation Center on Forecast and Evaluation of
11 Meteorological Disasters (CIC-FEMD), Nanjing University of Information Science &
12 Technology, Nanjing 210044, China.

13

14 ***Correspondence:** Yan-Lin Zhang (dryanlinzhang@outlook.com)

15

16 **Abstract.** Atmospheric low molecular weight amines play important roles in aerosol
17 physiochemical properties and climate. However, the compositions, sources, and
18 secondary formation mechanisms of amines in offshore aerosols remain unclear. Here,
19 an integrated observation of methylamine (MA), ethylamine (EA), dimethylamine
20 (DMA), iso-propanamine (IPA), propanamine (PA), “trimethylamine + diethylamine”
21 (TMDEA), and over 100 other chemical components was conducted in total
22 suspended particles samples collected during a spring 2018 research cruise across the
23 Yellow Sea and Bohai Sea, China. Concentrations of total amines exhibited a
24 north-to-south gradient from the Bohai Sea to the South Yellow Sea, corresponding to
25 the decreasing influence of terrestrial air masses. Source analyses of amines were
26 performed using specific organic molecular tracers representing primary biogenic
27 sources, higher plant waxes, marine/microbial sources, biogenic secondary organic
28 aerosols, biomass burning, and fossil fuel combustion, and two major secondary
29 formation pathways were inferred. MA, EA, and DMA were largely influenced by
30 terrestrial biogenic and anthropogenic sources, with the majority (74.0%, 52.6%, and
31 65.7%) formed via nitrate-associated secondary formation pathways. PA was mainly
32 derived from combustion-related sources along with terrestrial and marine biogenic
33 contributions. In contrast, the predominant TMDEA was mostly generated via
34 sulfate-associated secondary formation pathways (61.8%) and contributed by marine
35 emissions, resulting in spatial pattern distinct from other major amines and the
36 north-to-south increasing relative contributions of amines in aerosols. These results
37 highlight the impact of terrestrial emissions on offshore aerosol chemistry and the

38 importance of origins and multiphase chemistry of amines under varying ambient
39 conditions.
40

41 **1 Introduction**

42 Amines, derivatives of ammonia (NH_3) with one or more hydrogen atoms replaced by
43 alkyl or aryl groups, represent an important class of nitrogen-containing organic
44 compounds (Shen et al., 2023; Zhu et al., 2022; Liu et al., 2023). Low molecular
45 weight amines, such as methylamine (MA), dimethylamine (DMA), trimethylamine
46 (TMA), ethylamine (EA), diethylamine (DEA), and propanamine (PA), are the most
47 common and abundant atmospheric amines. They are ubiquitous in both the gas and
48 particle phases due to high water solubility and strong alkalinity (Ge et al., 2011b, a).
49 These amines are primarily emitted in the gas phase and mainly exist in aerosols as
50 aminium salts formed via chemically reactive gas-to-particle conversion, commonly
51 referred to as secondary formation of amines.

52 Gaseous amines can be oxidized by atmospheric oxidants (including OH, O_3 , and NO_x)
53 (Tang et al., 2013; Nielsen et al., 2012), and undergo gas-to-particle conversion
54 through direct dissolution (Liu et al., 2018), acid-base reactions (Liu et al., 2023;
55 Barsanti and Pankow, 2006; Chen et al., 2022), and heterogeneous reactions (Pankow,
56 2015; Chan and Chan, 2013; Qiu and Zhang, 2013), leading to the formation of
57 secondary organic aerosols (SOA) that aggravate air quality and visibility. Gaseous
58 amines and their oxidization products, such as nitrosamines, pose significant risks to
59 human health (Li et al., 2019a; Lee and Wexler, 2013). The multiphase chemistry of
60 atmospheric amines participates in and accelerates new particle formation (Liu et al.,
61 2022; Huang et al., 2022; Yao et al., 2018; Shen et al., 2019), enhances aerosol
62 hygroscopicity (Chu et al., 2015; Gomez-Hernandez et al., 2016), and promotes the

63 activation of cloud condensation nuclei (Tang et al., 2014; Corral et al., 2022;
64 Gomez-Hernandez et al., 2016). Additionally, amines can promote the formation of
65 brown carbon (Marrero-Ortiz et al., 2018; Lin et al., 2015), thereby affecting
66 atmospheric radiation and climate. However, challenges in detecting minute levels of
67 amines, the scarcity of ambient measurements, and a limited process-based
68 understanding of aerosol formation have led to the underrepresented of amines in
69 global climate models (Kanawade and Jokinen, 2025).

70 Atmospheric amines originate from diverse natural (e.g. ocean, soil, and vegetation)
71 and anthropogenic sources (e.g. animal husbandry, biomass burning, coal combustion,
72 vehicle emissions, composting, waste incineration, industrial activities, and sewage)
73 (Shen et al., 2017; Hemmilä et al., 2018; Feng et al., 2022). Ocean is an important
74 natural source of low molecular weight amines, with emissions mainly driven by
75 biological processes (Calderón et al., 2007; Wang and Lee, 1994). Global modeling
76 (Myriokefalitakis et al., 2010) suggested that amines contribute approximately 20% to
77 marine SOA, ranking second to dimethylsulfide (DMS). However, this contribution
78 may be substantially overestimated, given that the actual proportions of amines
79 relative to NH_3 are up to three orders of magnitude lower than the values assumed in
80 the model. Measured concentrations of amines vary across different oceans in both
81 seawater and the atmosphere (Violaki and Mihalopoulos, 2010; Gibb et al., 1999; Van
82 Neste et al., 1987). Elevated concentrations of DMA and TMA are associated with
83 marine biological activities (Carpenter et al., 2012; Welsh, 2000) and algal blooms
84 (Müller et al., 2009; Facchini et al., 2008b). Marine organisms act as both sources and

85 sinks of amines, and the source/sink capability of the ocean varies with ambient
86 conditions (Pinxteren et al., 2019). For instance, TMA can be released from living
87 tissues or during biodegradation and decay, and can also be utilized by
88 microorganisms for energy metabolism (Sun et al., 2019; Köllner et al., 2017; Lidbury
89 et al., 2015). TMA can be biologically oxidized to trimethylamine oxide (TMAO), an
90 osmotic regulatory compound in marine organisms and a precursor of DMA and MA
91 (Chen et al., 2011; Lidbury et al., 2017). The calculated sea-to-air fluxes of DMA at
92 Cape Verde were both positive and negative, whereas those of MA were mostly
93 positive (Pinxteren et al., 2019). Amines in marine aerosols are originated from sea
94 spray (Bates et al., 2012; Gorzelska and Galloway, 1990), bubble bursting (Milne and
95 Zika, 1993), and gas-to-particle conversion, i.e. secondary formation (Rinaldi et al.,
96 2010; Facchini et al., 2008b; Facchini et al., 2008a). Most low molecular weight
97 amines in marine aerosols are considered to be secondarily formed (Gaston et al.,
98 2013; Dall'osto et al., 2019). For instance, 11–25% of MA, DMA and TMA in the
99 Antarctic sympagic environment originated from primary marine aerosols, whereas
100 75–89% were incorporated into aerosols after air-sea exchange (Dall'osto et al., 2019).
101 Amines in marine aerosols may also be influenced by inland sources and long-range
102 atmospheric transportation (Nielsen et al., 2012). TMA detected in aerosols off the
103 coast of California was associated with inland animal husbandry activities rather than
104 local marine biogenic emissions (Gaston et al., 2013).

105 Atmospheric low molecular weight amines have been widely reported in urban
106 (Cheng et al., 2020; Chen et al., 2019; Liu et al., 2017), rural (Cheng et al., 2018; Lin

107 et al., 2017), and coastal areas (Liu et al., 2022; Hu et al., 2015; Zhou et al., 2019; Du
108 et al., 2021), but relatively few studies have focused on marine regions of China
109 (Zhou et al., 2019; Yu et al., 2016; Hu et al., 2015). The Yellow Sea (YS) and Bohai
110 Sea (BS) are two marginal seas in eastern China that serve as transition zones for
111 atmospheric pollutants and particles transported from East Asia to the Northwest
112 Pacific Ocean (NWPO). The YS is divided into South Yellow Sea (SYS) and North
113 Yellow Sea (NYS), both semi-open sea areas of the NWPO. The BS is the
114 northernmost marginal sea of China, surrounded by land on three sides and bordered
115 to the east by the NYS. Aerosols over the YS–BS are significantly influenced by the
116 transportation of terrestrial emissions from northern and eastern China during the
117 prevailing spring East Asia monsoon (Fang et al., 2016). Previous studies on aerosol
118 amines over the marginal seas of China have mainly focused on DMA and TMDEA,
119 the sum of TMA and DEA (Zhou et al., 2019; Xie et al., 2018; Yu et al., 2016; Hu et
120 al., 2015). Although MA has been observed as the dominant amine in urban aerosols
121 in northern China and the Yangtze River Delta region (Yang et al., 2023; Liu et al.,
122 2023; Huang et al., 2018), its contribution in marine aerosols of China remains
123 unclear. The primary sources and secondary formation pathways of aerosol amines
124 over the YS–BS are poorly constrained due to the combined influence of complex
125 terrestrial and marine emissions, as well as the lack of specific source indicators. To
126 address these, an integrated analysis of six major amines together with more than 100
127 other chemical components in aerosols was conducted using filter samples collected
128 over the YS–BS during a research cruise in spring 2018. Spatial variations, potential

129 sources, and secondary formation pathways of aerosol amines were investigated. By
130 elucidating the relationships between individual amines and specific organic
131 molecular tracers representing six source categories, this study provides new
132 observational constraints on the sources and atmospheric processes of amines in
133 marine aerosols. The results suggest that individual amines were associated with
134 different primary sources and likely underwent two distinct major secondary
135 formation pathways. These findings provide a basis for improving the quantitative
136 source apportionment of aerosol amines and for further clarify their origins and
137 gas-to-particle conversion under varying ambient conditions.

138

139 **2 Methods**

140 **2.1 Aerosol sampling**

141 During a Chinese oceanographic cruise over the YS–BS (28 March–16 April 2018),
142 total suspended particles (TSP) samples were collected on prebaked (450 °C for 6 h)
143 quartz fiber filters using a high-volume air sampler (ASM-1000, Guangzhou; flow
144 rate: 1 m³ min⁻¹) aboard the *Dong Fang Hong 2* (Figure S1 and Table S1). The
145 sampler was installed windward on the upper deck at the ship bow (~10 m above the
146 sea surface). To avoid contamination from the ship exhaust, sampling was performed
147 only while the vessel was underway. During the sampling period, a total of 15
148 samples were collected, and 3 field blank filters were prepared by collecting without
149 airflow. The samples were categorized into SYS, NYS, and BS by sampling positions.

150 Real-time navigation and meteorological data, including position (longitude and
151 latitude), ambient temperature (T), relative humidity (RH), and wind speed, were
152 recorded by the onboard monitoring system.

153

154 **2.2 Chemical analysis**

155 Low molecular weight amines can be directly separated and quantified using ion
156 chromatography methods (Feng et al., 2020; Place et al., 2017; VandenBoer et al.,
157 2012). Six major protonated amine species extracted from TSP filter samples,
158 including methylamine (CH_3NH_3^+ , MA), ethylamine ($\text{CH}_3\text{CH}_2\text{NH}_3^+$, EA),
159 dimethylamine [$(\text{CH}_3)_2\text{NH}_2^+$, DMA], iso-propanamine [$(\text{CH}_3)_2\text{CHNH}_3^+$, IPA],
160 propanamine ($\text{CH}_3\text{CH}_2\text{CH}_2\text{NH}_3^+$, PA), and the combined species “trimethylamine
161 [$(\text{CH}_3)_3\text{NH}^+$, TMA] + diethylamine [$(\text{CH}_3\text{CH}_2)_2\text{NH}_2^+$, DEA]” (TMDEA), were
162 measured by a ion chromatography (Thermo Fisher Scientific Dionex ICS-5000+), as
163 described in detail elsewhere (Yang et al., 2023). Before analysis, a 0.8 cm^2 portion of
164 each sampled or blank filter was ultrasonically extracted 3 times with 10–30 mL of
165 ultrapure water for 15 min in an ice-water bath, followed by filtration through a 0.22
166 μm Teflon filter. The analytical precision was better than 10%, and recoveries for all
167 amines ranged from 90% to 110%. The method detection limits (MDLs) for MA, EA,
168 DMA, IPA, PA, and TMDEA were 0.4 ng m^{-3} , 0.4 ng m^{-3} , 0.5 ng m^{-3} , 0.7 ng m^{-3} , 1.1
169 ng m^{-3} , and 2.9 ng m^{-3} , respectively.

170 To provide a comprehensive characterization of aerosols, other key chemical

171 components in TSP samples were also analyzed, including water-soluble inorganic
172 ions (WSIIs; Na^+ , NH_4^+ , K^+ , Mg^{2+} , Ca^{2+} , Cl^- , NO_3^- , SO_4^{2-} , etc.), low molecular
173 weight organic acids (CHO_2^- , $\text{C}_2\text{H}_3\text{O}_2^-$, $\text{C}_4\text{H}_4\text{O}_4^{2-}$, $\text{C}_5\text{H}_6\text{O}_4^{2-}$, $\text{CH}_3\text{O}_3\text{S}^-/\text{MSA}^-$, etc.),
174 carbonaceous components [Organic carbon (OC) and Elemental carbon (EC)], and
175 organic compositions (polar and nonpolar). Detailed methodologies for analyzing
176 these species had been described elsewhere (Fan et al., 2019; Cao et al., 2024), and
177 the measurement results were summarized in Table S2.

178

179 **2.3 Auxiliary data**

180 Average chlorophyll *a* (Chl *a*) concentrations in seawater during the sampling period
181 were retrieved from combined Aqua-MODIS and Terra-MODIS datasets
182 (<https://oceancolor.gsfc.nasa.gov/>) using ArcGIS software (Figure S2). Fire spot
183 information was obtained from the Fire Information for Resource Management
184 System (FIRMS, <https://firms.modaps.eosdis.nasa.gov/>). Based on the archived
185 Global Data Assimilation System (<ftp://arlftp.arlhq.noaa.gov/pub/archives/gdas1/>)
186 meteorological data, 48 h backward air-mass trajectories at 200 m above ground level
187 were calculated using the Hybrid Single-particle Lagrangian Integrated Trajectory
188 (HYSPLIT) model, and subsequently processed with MeteoInfo software (Figure S3).
189 The trajectories were calculated from the position and time point at the beginning of
190 each sampling, with hourly intervals thereafter.

191

192 **3 Results and discussion**

193 **3.1 Overview of amines in marine aerosols**

194 During the cruise over the YS–BS from 28 March to 16 April 2018, the
195 concentrations of total amines (Σ amines; the summation of MA, EA, DMA, IPA, PA,
196 and TMDEA) in TSP ranged from 16.2 ng m⁻³ to 89.1 ng m⁻³ (Figure 1). Lower
197 Σ amines concentrations were observed over the SYS and NYS, averaging 40.4 ± 16.4
198 ng m⁻³ and 43.5 ± 17.5 ng m⁻³, respectively, and higher concentrations occurred over
199 the BS, averaging at 63.6 ± 18.3 ng m⁻³. Concentrations of other chemical
200 components, including total WSIs, TC, and total measured organic compositions,
201 exhibited a similar spatial pattern (SYS < NYS < BS; Table S2).

202 TMDEA was the predominant amine species in TSP over the YS–BS, with
203 concentrations ranging from 6.1 ng m⁻³ to 36.3 ng m⁻³ (Figure S4) and averages of
204 20.7 ± 9.1 ng m⁻³, 17.8 ± 7.3 ng m⁻³, and 23.8 ± 3.7 ng m⁻³ over the SYS, NYS, and
205 BS, respectively. The fraction of TMDEA in Σ amines decreased from the SYS
206 (51.2%) to the NYS (40.8%) and BS (37.4%). The concentrations of amines measured
207 in TSP were comparable to those in PM_{2.5} and PM₁₀ (Table S3), as amines are
208 predominantly (> 70%) distributed in aerosols with diameters < 1.8 μm (Zhou et al.,
209 2019; Xie et al., 2018; Yu et al., 2016). Compared with other marine and coastal
210 regions, the aerosol TMDEA concentrations in spring over the YS–BS were higher
211 than those reported for the East China Sea (ECS), Huaniao Island (in the ECS), South
212 China Sea (SCS), and Northwest Pacific Ocean (NWPO) (Chen et al., 2022; Zhou et
213 al., 2019; Xie et al., 2018; Yu et al., 2016). Over the YS–BS, aerosol TMDEA

214 concentrations were higher in summer than in spring and autumn (Xie et al., 2018; Yu
215 et al., 2016).

216 MA, the second most abundant amine species (range: 0.9–44.0 ng m⁻³), exhibited
217 average concentrations of 22.8 ± 15.0 ng m⁻³ and 15.7 ± 7.7 ng m⁻³ in TSP over the
218 BS and NYS, contributing 35.9% to Σamines. Relatively lower MA concentrations
219 (10.0 ± 7.0 ng m⁻³) and a smaller proportion of MA to Σamines (24.9%) were
220 observed over the SYS compared with the NYS–BS. A markedly high MA
221 concentration was found in S14, the cruise track of which was close to land and
222 largely influenced by terrestrial air masses (Figure S3 and Figure S4). The average
223 aerosol MA concentration over the YS–BS in spring (13.7 ng m⁻³) was comparable to
224 that at Jeju Island, South Korea (Yang et al., 2004), and was higher than those at
225 coastal Qingdao (a port city surrounded by the YS and BS) and Huaniao Island in
226 winter (Liu et al., 2022; Huang et al., 2018). These values were further higher than
227 those reported for the Arabian Sea (Gibb et al., 1999) and tropical Atlantic (Pinxteren
228 et al., 2019), where measurements focused on ultrafine particles may underestimate
229 aerosol amines concentrations to some extent.

230 DMA concentrations ranged from 1.3 ng m⁻³ to 10.4 ng m⁻³, with averages of 3.5 ±
231 2.1 ng m⁻³, 3.8 ± 2.6 ng m⁻³, and 7.9 ± 2.1 ng m⁻³ in TSP over the SYS, NYS, and BS,
232 respectively. Higher DMA contributions to Σamines were found over the BS (12.4%)
233 than the NYS (8.7%) and SYS (8.6%). The average aerosol DMA concentration over
234 the YS–BS in spring (4.4 ng m⁻³) was much lower than those reported for coastal
235 Qingdao in winter and for the YS–BS in different seasons in previous years (Table

236 S3). EA ($0.6\text{--}4.8\text{ ng m}^{-3}$), IPA ($0.5\text{--}3.9\text{ ng m}^{-3}$), and PA ($1.3\text{--}5.1\text{ ng m}^{-3}$) constituted
237 a relatively small fraction of Σ amines ($7.3\text{--}28.2\%$), with average concentrations of
238 $2.0 \pm 1.2\text{ ng m}^{-3}$, $1.8 \pm 1.0\text{ ng m}^{-3}$, and $2.9 \pm 1.0\text{ ng m}^{-3}$ in TSP over the YS–BS,
239 respectively. The average aerosol EA concentration over the BS (3.0 ng m^{-3}) was
240 comparable to those observed at coastal Qingdao (Liu et al., 2022) and Jeju Island,
241 South Korea (Yang et al., 2004). Comparable data for EA, IPA, and PA concentrations
242 in marine aerosols were currently limited.

243 According to air-mass analyses (Figure S3), S3 and S12–19 (include all samples from
244 the NYS–BS) were strongly influenced by continental outflow, while S5, S6, and S8
245 (from the SYS) were dominated by marine air masses. The remaining samples were
246 affected by mixed terrestrial and marine air masses. Higher concentrations of MA
247 ($16.0 \pm 11.5\text{ ng m}^{-3}$), EA ($2.3 \pm 1.4\text{ ng m}^{-3}$), DMA ($5.3 \pm 2.9\text{ ng m}^{-3}$), and PA ($3.2 \pm$
248 1.0 ng m^{-3}) were observed in samples influenced by continental outflow compared to
249 those dominated by marine air masses (MA: $10.0 \pm 6.6\text{ ng m}^{-3}$; EA: $1.3 \pm 0.2\text{ ng m}^{-3}$;
250 DMA: $2.0 \pm 0.1\text{ ng m}^{-3}$; and PA: $2.3 \pm 1.0\text{ ng m}^{-3}$). In contrast, TMDEA
251 concentrations were higher in samples dominated by marine air masses ($27.6 \pm 9.1\text{ ng}$
252 m^{-3}) than those influenced by continental outflow ($19.8 \pm 7.4\text{ ng m}^{-3}$). Strong positive
253 correlations were observed among MA, EA, and DMA ($R = 0.73\text{--}0.77$, $P < 0.01$),
254 whereas no statistically significant correlation ($P > 0.05$) exhibited between IPA, PA,
255 or TMDEA and other amine species. These results suggested that MA, EA, and DMA
256 might share similar sources and secondary formation pathways, whereas IPA, PA, and
257 TMDEA were likely influenced by different sources or atmospheric processes.

258

259 **3.2 Relative contributions of amines in TSP over the YS–BS**

260 Amines, as a subset of water-soluble organic carbon, generally constitute only a minor
261 fraction of OC. Both OC and EC concentrations in TSP increased from the SYS to the
262 NYS and BS (Figure 2), consistent with the strengthened influence of atmospheric
263 pollutants transported from mainland East Asia (Figure S3). However, the
264 \sum amines-C/OC ratios (2.1–8.8‰) were relatively higher in aerosols over the SYS (5.4
265 $\pm 2.2\%$) than the NYS ($4.4 \pm 1.7\%$) and BS ($4.0 \pm 1.4\%$; Figure S5), contrary to the
266 spatial variation of \sum amines concentrations.

267 Positive correlations were found between NH_4^+ and amines, including MA ($R = 0.78$,
268 $P < 0.01$), DMA ($R = 0.74$, $P < 0.01$), EA ($R = 0.57$, $P < 0.05$), PA ($R = 0.58$, $P < 0.05$),
269 and TMDEA ($R = 0.52$, $P < 0.05$). Aerosol NH_4^+ is formed via the heterogeneous
270 uptake of NH_3 , the most abundant alkaline gas in the atmosphere, by acidic aerosols,
271 and exists as ammonium sulfate $[(\text{NH}_4)_2\text{SO}_4]$, ammonium bisulfate (NH_4HSO_4),
272 ammonium nitrate (NH_4NO_3), and ammonium chloride (NH_4Cl) (Behera et al., 2013).
273 Atmosphere NH_3 shares overlapping source profiles with gaseous amines, including
274 animal husbandry, biomass burning, vehicle emissions, industrial activities, soil, and
275 the ocean. This was inferred as the reason for considerable correlations between NH_4^+
276 and amines in aerosols.

277 Gaseous low molecular weight amines are more alkaline than NH_3 , and may compete
278 with NH_3 in atmospheric acid-base reactions (Sorooshian et al., 2008; Chen et al.,

279 2022). The molar ratios of aerosol amines to NH_4^+ were calculated to assess their
280 relative contributions to the neutralization of acidic species in aerosols (Hu et al.,
281 2015). The $\sum\text{amines}/\text{NH}_4^+$ molar ratios (4.8–17.0‰) were $9.7 \pm 3.4\%$, $7.6 \pm 0.8\%$,
282 and $6.8 \pm 1.8\%$ over the SYS, NYS, and BS, respectively. The spatial pattern of
283 $\sum\text{amines}/\text{NH}_4^+$ molar ratios (SYS > NYS > BS) was consistent with that of the
284 $\sum\text{amines-C}/\text{OC}$ ratios, both indicating a north-to-south increase in the relative
285 contributions of amines to aerosol composition over the YS–BS.

286 The $\sum\text{amines}/\text{NH}_4^+$ molar ratios obtained in this study were of the same order of
287 magnitude as those reported previously (Xie et al., 2018; Yu et al., 2016). Overall,
288 amines contribute negligibly to the neutralization of acidic species in TSP compared
289 with NH_4^+ , which is reasonable given the much higher atmospheric abundance of NH_3
290 relative to gaseous amines (Zheng et al., 2015; You et al., 2014; Ge et al., 2011a, b).
291 However, amines potentially play a more important role in neutralizing acidic species
292 in submicron particles, particularly in the presence of organic compounds (Xie et al.,
293 2018). The composition of NH_4^+ , NO_3^- , and SO_4^{2-} may influence aerosol amines, as
294 they can act as competitors for neutralization and as major reactants in aerosol
295 formation. The $\text{NH}_4^+(\text{Cl}^- + \text{NO}_3^- + 2\times\text{SO}_4^{2-})$ molar ratios is commonly used to
296 assess whether NH_4^+ fully neutralizes acidic species (Cl^- , NO_3^- , and SO_4^{2-}) in
297 aerosols. In this study, the ratios in TSP over the YS–BS were mostly < 1 (0.8 ± 0.2 ;
298 Figure 2 and Figure S5), indicating NH_4^+ deficiency. This deficiency was more
299 markedly over the BS (0.6 ± 0.0) than the YS (0.8 ± 0.2). The $\text{NO}_3^-/\text{SO}_4^{2-}$ molar
300 ratios in TSP over the SYS (0.8 ± 0.8) were significantly lower than those over the

301 NYS (2.3 ± 0.4) and NYS (2.3 ± 0.4) and BS (2.5 ± 0.8), indicating that SO_4^{2-} was the
302 dominate acidic species in SYS aerosols, whereas NO_3^- dominated in NYS and BS
303 aerosols. The composition of NH_4^+ , NO_3^- , and SO_4^{2-} in NYS aerosols was
304 intermediate between that over the BS and SYS, consistent with the regional
305 variations in amines concentrations and composition. Molar concentrations of
306 \sum amines increased with increasing NH_4^+ deficiency [indicated by $\text{NH}_4^+ / (\text{Cl}^- + \text{NO}_3^-$
307 $+ 2 \times \text{SO}_4^{2-})$ molar ratios; $R = -0.57$, $P < 0.05$] and with $\text{NO}_3^- / \text{SO}_4^{2-}$ ratios ($R = 0.56$,
308 $P < 0.05$), particularly in BS aerosols. Nevertheless, individual amines responded
309 differently to variations in NH_4^+ deficiency and $\text{NO}_3^- / \text{SO}_4^{2-}$ molar ratios, likely
310 reflecting differences in their primary sources (terrestrial vs. marine) and formation
311 pathways (nitrate vs. sulfate associated).

312

313 **3.3 Source analysis of amines in TSP over the YS–BS**

314 **3.3.1 Biogenic sources**

315 On a global scale, ocean is a major source of gaseous methylamines (fluxes: TMA >
316 MA >> DMA) (Van Neste et al., 1987; Schade and Crutzen, 1995). Intensive ocean
317 farming is widespread in the coastal areas of the YS–BS (Hu et al., 2015), where
318 marine biogenic sources, including fish emission (Namieśnik et al., 2003),
319 biodegradation of nitrogen-containing materials, and decay process (Calderón et al.,
320 2007) may release gaseous amines into the atmosphere. The concentration of Chl *a* in
321 surface seawater is an indicator of phytoplankton biomass and thus reflects the

322 intensity of marine biogenic emissions to some extent. Significantly higher Chl *a*
323 concentrations were observed in the BS than in the YS, with relatively elevated values
324 in near shore areas (Figure S2). The spatial distribution of Σ amines in TSP over the
325 YS–BS was broadly consistent with, though not identical to, Chl *a* concentrations in
326 surface seawater. This discrepancy likely reflected secondary formation of amines in
327 aerosols, as well as the influence of long-range transportation of terrestrial emissions
328 driven by the prevailing East Asia monsoon during spring, particularly to S3 and
329 S12–19 (Figure S3).

330 Aerosol MA, EA, and DMA exhibited positive linear relationships with total primary
331 sugars and sugar alcohols (Figure 3 a–c and Table S4), which mainly originate from
332 primary biogenic sources such as bacteria, pollen, and plant or animal debris (Li et al.,
333 2019b). These sources can be either marine or terrestrial. Fungal spore OC and plant
334 debris OC were estimated from mannitol and arabitol (Bauer et al., 2008), and glucose
335 (Zheng et al., 2018), respectively. Significant positive correlations were observed
336 between MA, EA, and DMA and fungal spore OC, plant debris OC, and several
337 individual primary sugars and sugar alcohols (e.g., trehalose, α -fructose, and sucrose;
338 $R > 0.50$, $P < 0.05$). DMA exhibited the strongest correlation with trehalose ($R = 0.71$,
339 $P < 0.01$), a compound abundant in microorganisms, algae, plants, and invertebrates,
340 and also acts as an indicator of re-suspended dust (Medeiros et al., 2006; Simoneit et
341 al., 2004). In addition, MA, DMA, and PA were positively correlated with high
342 molecular weight *n*-alkanes (ALK_{HMW} ; C_{27} , C_{29} , C_{31} and C_{33}) and fatty alcohols
343 (ALC_{HMW} ; $> C_{19alc}$; Figure 3 d–e), while PA also correlated with low molecular

344 weight fatty acids (FA_{LMW} ; $\leq C_{19:0}$; Figure 3 f). ALK_{HMW} (Rogge et al., 1993),
345 ALC_{HMW} (Simoneit et al., 1991), and high molecular weight fatty acids (FA_{HMW} ; $>$
346 $C_{19:0}$) are tracers of higher plant waxes from terrestrial vegetation, whereas FA_{LMW} are
347 associated with marine/microbial sources (Haque et al., 2019). Overall, these findings
348 indicated that amines (MA, EA, DMA, and PA) in TSP over the YS–BS were
349 contributed by biogenic sources. MA and DMA were largely influenced by terrestrial
350 biogenic emissions, whereas PA was affected by both terrestrial and marine biogenic
351 sources.

352 Atmospheric biogenic secondary organic aerosols (BSOA) are formed via the
353 photochemical oxidation of biogenic volatile organic compounds (BVOCs) by O_3 ,
354 OH and NO_x (Ng et al., 2011). In this study, six isoprene SOA (SOA_I) tracers, three
355 monoterpene SOA (SOA_M) tracers, and one β -caryophyllene SOA (SOA_C) tracer were
356 measured in TSP over the YS–BS. Biogenic SOC derived from isoprene,
357 monoterpene, and β -caryophyllene was estimated using the tracer-based method
358 (Kang et al., 2018; Kleindienst et al., 2007). Significant positive linearity were
359 observed between MA and both isoprene and monoterpene SOC (Figure 3 g–h).
360 Among the SOA_I tracers, MA exhibited stronger correlations with 2-methyltetrols
361 (2-MTLs; $R = 0.74$, $P < 0.01$) and C_5 -alkene triols ($R = 0.66$, $P < 0.01$) than with
362 2-methylglyceric acid (2-MGA; $R = 0.64$, $P < 0.05$). DMA was also positively
363 correlated with isoprene SOC ($R = 0.55$, $P < 0.05$), only driven by its association with
364 2-MTLs ($R = 0.59$, $P < 0.05$). Among the SOA_M tracers, pinonic acid correlated with
365 MA ($R = 0.73$, $P < 0.01$), EA ($R = 0.52$, $P < 0.05$), and DMA ($R = 0.58$, $P < 0.05$),

366 while pinic acid only correlated with MA ($R = 0.59$, $P < 0.05$). In addition, PA showed
367 a positive linearity with β -caryophyllene SOC ($R = 0.67$, $P < 0.01$; Figure 3 i). These
368 findings supported that MA, EA, DMA, and PA shared common sources with BVOCs
369 and/or interacted with BSOA formation processes. High concentrations of amines and
370 biomarkers were simultaneously observed in aerosols over the BS and NYS, whereas
371 amines in the SYS aerosols remained at moderate levels despite low tracers
372 concentrations (Figure 3). These indicated that terrestrial biogenic emissions
373 contributed more substantially to aerosol amines over the BS and NYS than the SYS.

374

375 3.3.2 Anthropogenic sources

376 Anthropogenic sources are another important contributor to atmospheric amines and
377 can be broadly categorized into combustion-related sources (e.g., biomass burning,
378 coal combustion, vehicle emissions, and waste incineration) and non-combustion
379 sources (e.g., animal husbandry, composting, industrial activities, sewage, and septic
380 system). EA ($R = 0.61$, $P < 0.05$) and DMA ($R = 0.72$, $P < 0.01$) concentrations in TSP
381 over the YS–BS increased with EC, indicating the influence of combustion emissions.
382 Levoglucosan (Lev) is a well-established tracer for biomass burning (Li et al., 2019b).
383 Concentrations of Lev derived from biomass burning (Lev_{bb}) were estimated using
384 Lev and non-sea-salt K^+ ($nss-K^+ = K^+ - 0.037 \times Na^+$) with considering its
385 atmospheric degradation and ~25% non-biomass burning sources [$Lev_{bb} = 0.75 \times Lev$
386 $\times nss-K^+ / (0.18 \times Lev + 0.08 \times nss-K^+)$]. Biomass burning was not a major source of

387 MA, EA, and DMA in aerosols over the YS–BS (Figure 3 j), but contributed
388 substantially to PA, as indicated by the positive linear relationships between PA and
389 both Lev_{bb} and lignin products (Figure 3 k–l). The most notable contributor to PA
390 from biomass burning was conifer burning (the second-largest portion of total
391 biomass burning) according to the correlations between PA and individual lignin
392 products, including 4-hydroxybenzoic acid (4-HBA; a herbaceous burning marker and
393 the predominate lignin product in this study; $R = 0.52$, $P < 0.05$), vanillic acid (VA; a
394 softwood and hardwood burning marker; $R = 0.67$, $P < 0.01$), syringic acid (SA; also
395 indicative of softwood and hardwood burning; $R = 0.60$, $P < 0.05$), and
396 dehydroabietic acid (DA; a conifer burning marker; $R = 0.71$, $P < 0.01$). In addition,
397 MA ($R = 0.57$, $P < 0.05$) and DMA ($R = 0.54$, $P < 0.05$) were positively correlated
398 with polycyclic aromatic hydrocarbons (PAHs), indicating potential contributions
399 from fossil fuel combustion (Table S4). Among all amines, PA showed the strongest
400 association with combustion-related sources, as evidenced by its correlations with
401 multiple fossil fuel combustion tracers (Figure 3 m–o), including low molecular
402 weight n-alkanes (ALK_{LMW} ; C_{20} – C_{26} ; $R = 0.67$, $P < 0.01$), PAHs ($R = 0.63$, $P < 0.05$),
403 hopanes ($R = 0.55$, $P < 0.05$), and steranes ($R = 0.57$, $P < 0.05$).

404 Emissions of amines (MA, DMA, and TMA) from non-combustion anthropogenic
405 sources, including composting, sewage, and septic systems, are largely linked to
406 biodegradation process. Therefore, the contribution of non-combustion anthropogenic
407 sources to amines was encompassed within the primary biogenic sources category.

408 IPA did not show any correlation with organic molecular tracers in TSP over the

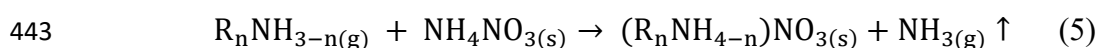
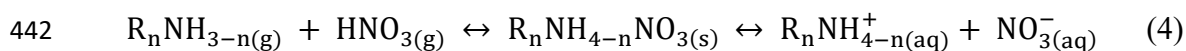
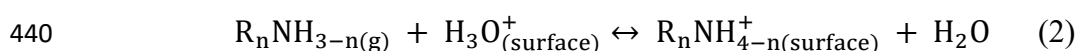
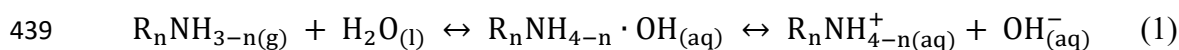
409 YS–BS. Given its widespread industrial use (e.g., in pesticides, pharmaceuticals, dye
410 intermediates, emulsifiers, detergents, surfactants, and textile additives), aerosol IPA
411 may be emitted in particulate form from specific industrial activities (Ge et al.,
412 2011a).

413

414 3.3.3 Secondary formation of MA, EA, DMA, and PA

415 Significant correlations were observed between MA, EA, DMA, and PA with Cl^- and
416 NO_3^- (Figure 4). The regression intercepts of MA, EA, and DMA against Cl^- or NO_3^-
417 were lower than those with primary organic tracers (Figure 3 and Figure S6),
418 indicating substantial contributions from secondary formation. Gas-to-particle
419 conversion of MA, EA, DMA, and PA was inferred to include direct dissolution
420 (Equation 1), uptake onto acidic particle surfaces (Equation 2) (Yin et al., 2011),
421 acid-base reactions (Equation 3–4), and displacement reactions with NH_4NO_3
422 (Equation 5) (Bzdek et al., 2010). For MA, EA, and DMA with high water solubility,
423 direct dissolution is considered as a key step in their gas-to-particle conversion.
424 Uptake of gaseous amines onto acidic particle surfaces was more important over the
425 BS, where aerosol acidic species are significantly in excess relative to NH_4^+ . MA, EA,
426 DMA, and PA in TSP over the YS–BS were formed via acid-base reactions with
427 atmospheric HCl and HNO_3 , while CH_3COOH also contributed to the formation of
428 aerosol MA, EA and DMA (Figure 4). In TSP over the YS–BS, NO_3^- concentrations
429 were significantly higher than those of Cl^- and $\text{C}_2\text{H}_3\text{O}_2^-$ (Table S2), thus, acid-base

430 reactions with HNO₃, together with displacement reactions involving NH₄NO₃, were
 431 the major pathways for the secondary formation of aerosol MA, EA, DMA and PA.
 432 The partitioning of amines into aerosols was further promoted by low T, high aerosol
 433 acidity, and high RH under dynamic solid/aqueous/gas equilibrium conditions. During
 434 the cruise, lower average T were observed over the BS (9.0°C) and NYS (6.7°C) than
 435 the SYS (9.5°C), and RH remained at a high level across the YS–BS (mean: 86.2%;
 436 median: 87.6%). The relatively abundant acidic species and lower T over the BS and
 437 NYS favored the partitioning of MA, EA, DMA, and PA into the particle phase
 438 compared with the conditions over the SYS.



444 Contributions of nitrate-associated secondary formation to aerosol amines were
 445 estimated from the average amine concentrations weighted by NO₃⁻ concentrations
 446 and regression intercepts (Figure S6). These estimates are semi-quantitative and
 447 limited by the small sample sizes, rather than representing quantitative source
 448 apportionment or mechanistic yields. Contributions of nitrate-associated secondary
 449 formation to \sum amines were highest in TSP over the BS (43.0 ± 26.9%), followed by
 450 the NYS (33.8 ± 19.7%) and SYS (21.8 ± 18.8%). Among individual amines,
 451 nitrate-associated secondary formation contributed most to MA (74.0 ± 61.5%),

452 followed by DMA ($65.7 \pm 44.3\%$), EA ($52.6 \pm 55.0\%$), and PA ($35.1 \pm 22.4\%$). PA
453 was less contributed by secondary formation, likely because it can be directly emitted
454 in particulate form or condense into aerosols after emission due to its relatively higher
455 boiling point (47.8°C) compared with MA (-6.3°C), EA (16.6°C), and DMA (7.4°C).

456 The relationships among amines (MA, EA, DMA, and PA), BSOA, and NO_3^- in TSP
457 over the YS–BS suggested potential interactions among their secondary formation
458 processes. NO_x , emitted from soil, biogenic activities, and combustion sources, are
459 important precursors for both BSOA and atmospheric HNO_3 , which subsequently
460 forms nitrate aerosols. This was supported by significant positive correlations
461 between NO_3^- and SOA_I ($R = 0.88$, $P < 0.01$), SOA_M ($R = 0.86$, $P < 0.01$), and SOA_C
462 ($R = 0.64$, $P < 0.05$). The formation of MA and DMA in aerosols might occur under
463 low NO_x conditions, as evidenced by their stronger correlations with 2-MTLs or
464 C_5 -alkene triols (products of isoprene photochemical oxidation under low NO_x
465 conditions) (Zheng et al., 2018; Zhang et al., 2011) than with 2-MGA (products of
466 isoprene aqueous-phase oxidation under high NO_x conditions) (He et al., 2018).

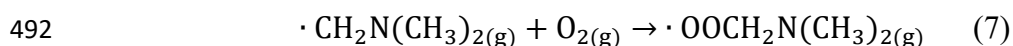
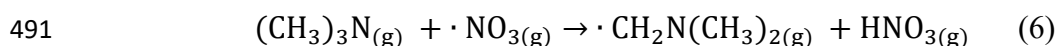
467 Strong atmospheric photo-oxidation generally accelerates the gas-phase degradation
468 of amines (Lee and Wexler, 2013), thereby reducing the formation of particle-phase
469 aminium salts. BVOCs, as precursors of BSOA, can generate HNO_3 via the “ $\text{NO}_3 +$
470 HC ” pathway, further promoting the formation of aminium nitrates. Meanwhile,
471 BSOA formation consumes atmospheric oxidants, which may reduce the degradation
472 of gaseous amines. The presence of an organic phase also enhances the
473 competitiveness of amines relative to NH_4^+ in aerosols (Xie et al., 2018). In addition,

474 the gas-to-particle conversion of amines may facilitate BSOA formation by providing
475 more hygroscopic particulate surfaces.

476

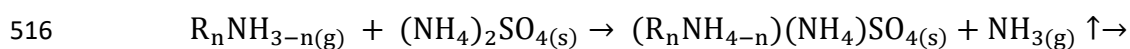
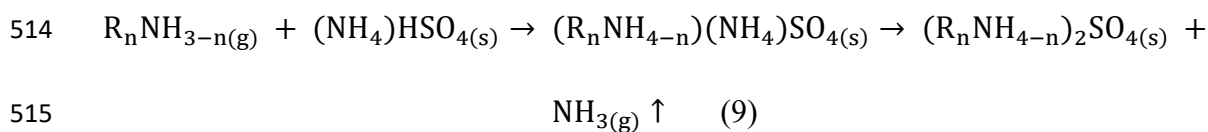
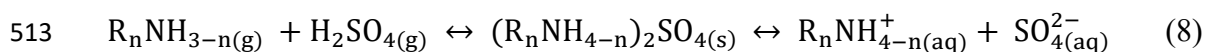
477 3.3.4 Secondary formation of TMDEA

478 Compared with other amines, a larger fraction of TMDEA likely originated from
479 marine sources, as evidenced by its relatively high concentrations and proportions in
480 TSP over the SYS, especially in samples dominated by marine air masses. Previous
481 studies also suggested marine emissions as an important potential source of TMDEA
482 (Schade and Crutzen, 1995; Pinxteren et al., 2019). TMDEA in TSP over the YS–BS
483 exhibited no correlation with organic molecular tracers representing primary biogenic
484 sources or BSOA (Table S4), although terrestrial vegetation and non-combustion
485 anthropogenic sources are also potential sources of gaseous TMDEA (Zhu et al., 2022;
486 Ge et al., 2011a). Concentrations of aerosol TMDEA were likely constrained by
487 gas-to-particle conversion efficiency. A hypothesis is that part of gaseous TMA
488 emitted from primary sources is consumed through reactions with NO₃ to form
489 non-aminium-salt SOA (Price et al., 2016; Price et al., 2014) and HNO₃ (Equation 6–
490 7).



493 TMDEA in TSP over the YS–BS showed no correlation with Cl⁻, or NO₃⁻, but
494 exhibited significant positive linear relationships with SO₄²⁻, C₄H₄O₄²⁻, and C₅H₆O₄²⁻

495 (Figure 4 and Figure S6). The gas-to-particle conversion of TMDEA was inferred to
 496 include uptake onto acidic particle surfaces (Equation 2), acid-base reactions with
 497 H₂SO₄ (Equation 8) and dicarboxylic acids (C₄H₆O₄ and C₅H₈O₄), as well as
 498 displacement reactions with (NH₄)HSO₄ and (NH₄)₂SO₄ (Equation 9–10). Uptake
 499 onto acidic particle surfaces is considered as a key step in the gas-to-particle
 500 conversion of TMDEA, as TMA exhibits the strongest alkalinity among gaseous
 501 amines. TMDEA in TSP over the YS–BS showed limited association with chloride
 502 and nitrate, likely due to the much lower competitiveness of TMA in forming these
 503 salts (as reflected by dissociation constants) relative to MA, EA, DMA, and NH₃ (Ge
 504 et al., 2011b). Instead, acid-base reactions with H₂SO₄, together with displacement
 505 reactions involving (NH₄)HSO₄ and (NH₄)₂SO₄, were the major pathways for the
 506 secondary formation of aerosol TMDEA. Contributions of dicarboxylic acids were
 507 relatively minor, given the significantly lower concentrations of C₄H₄O₄²⁻ and
 508 C₅H₆O₄²⁻ compared with SO₄²⁻ in TSP over the YS–BS (Table S2). These findings
 509 were consistent with previous laboratory and theoretical studies showing that TMA
 510 preferentially reacts with H₂SO₄ (Johnson and Jen, 2023), and that DEA exhibits the
 511 highest uptake coefficient during the irreversible reactive uptake of gaseous
 512 ethylamines by H₂SO₄ (Yin et al., 2011).



517 $(R_n\text{NH}_{4-n})_2\text{SO}_{4(s)} + \text{NH}_{3(g)} \uparrow$ (10)

518 Sulfate-associated secondary formation contributed $61.8 \pm 31.6\%$ to TMDEA in TSP
519 over the YS–BS, as estimated from average TMDEA concentrations weighted by
520 SO_4^{2-} concentrations and regression intercept (Figure S6). The contributions were
521 highest over the SYS ($63.4 \pm 36.2\%$), followed by the BS ($61.4 \pm 16.2\%$) and NYS
522 ($55.8 \pm 29.3\%$). Correspondingly, sulfate-associated secondary formation contributed
523 $23.0 \pm 6.0\%$, $22.8 \pm 13.7\%$, and $32.5 \pm 22.1\%$ to $\sum\text{amines}$ over the BS, NYS, and
524 SYS, respectively. The spatial pattern of average contributions from sulfate-associated
525 secondary formation (SYS > BS > NYS) was consistent with that of T, indicating that
526 T conditions influenced the relative advantages of sulfate and nitrate formation.

527 Significant positive correlations were observed between dicarboxylates ($\text{C}_4\text{H}_4\text{O}_4^{2-}$ and
528 $\text{C}_5\text{H}_6\text{O}_4^{2-}$; $R = 0.78$ and 0.66 , $P < 0.01$) and non-sea-salt sulfate ($\text{nss-SO}_4^{2-} = \text{SO}_4^{2-} -$
529 $0.2516 \times \text{Na}^+$), indicating that these species shared similar potential terrestrial
530 anthropogenic or marine biogenic origins (Miyazaki et al., 2010; Mochida et al.,
531 2003). Molar concentrations of biogenic- SO_4^{2-} were estimated from T and MSA^- , as
532 both MSA^- and SO_4^{2-} are oxidation products of DMS emitted from marine biogenic
533 sources (Nakamura et al., 2005; Bates et al., 1992). Anthropogenic- SO_4^{2-} was then
534 calculated by nss-SO_4^{2-} subtracting biogenic- SO_4^{2-} . The result showed that
535 biogenic- SO_4^{2-} accounted for 11.1% of total SO_4^{2-} in TSP over the SYS, markedly
536 higher than the NYS (4.3%) and BS (2.1%), yet still representing a minor fraction
537 relative to anthropogenic- SO_4^{2-} . Consequently, TMDEA in TSP over the YS–BS was
538 predominantly taken up by anthropogenic sulfate aerosols.

539 High concentrations of TMDEA, SO_4^{2-} , $\text{C}_4\text{H}_4\text{O}_4^{2-}$, and $\text{C}_5\text{H}_6\text{O}_4^{2-}$ were simultaneously
540 observed in S5 and S6 over the SYS, along with relatively high marine biogenic
541 contributions (Biogenic- $\text{SO}_4^{2-}/\text{SO}_4^{2-}$: 11.2% and 10.3%). NH_4^+ deficiency [$\text{NH}_4^+ / (\text{Cl}^-$
542 $+ \text{NO}_3^- + 2 * \text{SO}_4^{2-})$]: 0.8 and 0.6], high T (12.2°C and 12.1°C), high wind speed (6.9 m
543 s^{-1} and 7.2 m s^{-1}), and saturated humidity (RH = 100%) were also found in S5 and S6
544 (Table S1). Under high RH, more amines partition into aqueous aerosols via direct
545 dissolution, promoting aminium salts formation, whereas high T shifts the
546 solid/aqueous/gas equilibrium of aminium salts toward the gas phase. Compared with
547 the chlorides and nitrates of MA, EA, DMA, and PA, TMDEA sulfates are more
548 thermally stable. In addition, strong winds enhance the emission of primary marine
549 aerosols from sea spray and bubble bursting, providing additional amines to TSP, as
550 amines are present in both seawater and primary marine aerosols. The source
551 contributions and major secondary formation pathways of amines were summarized in
552 Figure 5.

553

554 **4 Conclusions**

555 This study systematically analyzed the spatial variations, potential sources, and
556 secondary formation mechanisms of six major low molecular weight amines in
557 aerosols over the marginal seas of China. Concentrations of total amines, water
558 soluble inorganic ions, carbonaceous components, and more than 100 organic
559 compositions generally exhibited a north-to-south decreasing pattern from the BS to

560 the NYS and SYS. This trend was consistent with the decreasing influence of
561 continental emissions from mainland East Asia, coupled with the increasing
562 contribution of the marine atmosphere.

563 Offshore aerosols exhibited distinct compositions of amines compared to terrestrial
564 aerosols, with TMDEA surpassing MA as the predominant amine. The proportions of
565 TMDEA in Σ amines and the relative contributions of Σ amines in aerosols increased
566 from north to south (BS < NYS < SYS), highlighting the ocean as a substantial source
567 of amines, particularly TMDEA, despite the significant influence of terrestrial
568 emissions. Distinct potential sources and major secondary formation pathways were
569 identified for different amine species. MA, EA, and DMA were mainly derived from
570 terrestrial biogenic and non-combustion anthropogenic sources, followed by fossil
571 fuel combustion, with over 50% formed via nitrate-associated secondary formation
572 pathways, interacting with BSOA formation in the NO_x -involved oxidation of BVOCs.
573 In comparison, PA was mainly originated from combustion-related sources along with
574 terrestrial and marine biogenic sources, with only ~35% contributed by
575 nitrate-associated secondary formation. In contrast to other amines, TMDEA was
576 mostly (~60%) generated via sulfate-associated secondary formation pathways, and
577 also contributed by primary marine aerosols from sea spray and bubble bursting.

578 Terrestrial sources not only emit gaseous amines but also contribute acidic aerosols
579 that can further uptake amines from marine sources during the transportation of air
580 masses from the mainland to the ocean. This process affects the physiochemical
581 properties and climate effects of marine aerosols, as well as the carbon and nitrogen

582 cycles. In addition to precursors abundance, ambient conditions also influence the
583 secondary formation of aerosol amines, leading to temporal and spatial variations in
584 their concentrations and compositions. Overall, our findings improve the
585 understanding of amines in marine aerosols, highlight the impact of terrestrial
586 emissions on offshore aerosol chemistry, and underscore the importance of multiphase
587 chemical processes of amines under diverse ambient conditions.

588

589 *Data availability.* Data are available from the corresponding author on request
590 (dryanlinzhang@outlook.com).

591

592 *Supplement.* The supplement related to this article is available online at: .

593

594 *Author contributions.* Xiao-Ying Yang wrote the draft and produced all the figures and
595 tables. Fang Cao, Yu-Chi Lin, and Yan-Lin Zhang provided useful comments and
596 revised the paper. Chang-Liu Wu, Yu-Xian Zhang, and Wen-Huai Song provided the
597 measurement data.

598

599 *Competing interests.* The authors declare that they have no conflict of interest.

600

601 *Acknowledgements.* We sincerely thank the captain and all crews of the *Dong Fang*

602 *Hong 2*; Wen-shuai Li and Tian-tian Liu from the Ocean University of China for their
603 help in the research cruise; Yi-xuan Zhang, Yan Fang, Sheng-cheng Shao, Xia Wu and
604 Tong Huang from Nanjing University of Information Science & Technology for their
605 assistance in the aerosol sampling and experiment process.

606

607 *Financial support.* This study was financially supported by National Natural Science
608 Foundation of China (No. 42325304 and 41977185).

609

610 **References**

611 Barsanti, K., and Pankow, J.: Thermodynamics of the formation of atmospheric organic particulate
612 matter by accretion reactions – Part 3: Carboxylic and dicarboxylic acids, *Atmospheric*
613 *Environment*, 40, 6676-6686, <https://doi.org/10.1016/j.atmosenv.2006.03.013> , 2006.

614 Bates, T., Calhoun, J., and Quinn, P.: Variations in the methanesulfonate to sulfate molar ratio in
615 marine aerosol particles over the South Pacific Ocean, *Journal of Geophysical Research*, 97,
616 9859-9865, <https://doi.org/10.1029/92JD00411> , 1992.

617 Bates, T. S., Quinn, P. K., Frossard, A. A., Russell, L. M., Hakala, J., Petäjä, T., Kulmala, M.,
618 Covert, D. S., Cappa, C. D., Li, S. M., Hayden, K. L., Nuaaman, I., McLaren, R., Massoli, P.,
619 Canagaratna, M. R., Onasch, T. B., Sueper, D., Worsnop, D. R., and Keene, W. C.: Measurements
620 of ocean derived aerosol off the coast of California, *Journal of Geophysical Research:*
621 *Atmospheres*, 117, (D21), <https://doi.org/10.1029/2012jd017588> , 2012.

622 Bauer, H., Claeys, M., Vermeylen, R., Schüller, E., Weinke, G., Berger, A., and Puxbaum, H.:
623 Arabitol and mannitol as tracers for a quantification of airborne fungal spores, *Atmospheric*
624 *Environment*, 42, 588-593, <https://doi.org/10.1016/j.atmosenv.2007.10.013> , 2008.

625 Behera, S. N., Sharma, M., Aneja, V. P., and Balasubramanian, R.: Ammonia in the atmosphere: a
626 review on emission sources, atmospheric chemistry and deposition on terrestrial bodies,

627 Environmental Science and Pollution Research, 20, 8092-8131,
628 <https://doi.org/10.1007/s11356-013-2051-9>, 2013.

629 Bzdek, B., Ridge, D., and Johnston, M.: Amine exchange into ammonium bisulfate and
630 ammonium nitrate nuclei, Atmospheric Chemistry and Physics, 10, 45-68,
631 <https://doi.org/10.5194/acp-10-3495-2010>, 2010.

632 Calderón, S., Poor, N., and Campbell, S.: Estimation of the particle and gas scavenging
633 contributions to wet deposition of organic nitrogen, Atmospheric Environment, 41, 4281-4290,
634 <https://doi.org/10.1016/j.atmosenv.2006.06.067>, 2007.

635 Cao, F., Zhang, Y.-X., Zhang, Y.-L., Song, W.-H., Zhang, Y.-X., Lin, Y.-C., Gul, C., and Haque, M.
636 M.: Molecular compositions of marine organic aerosols over the Bohai and Yellow Seas: Influence
637 of primary emission and secondary formation, Atmospheric Research, 297, 107088,
638 <https://doi.org/10.1016/j.atmosres.2023.107088>, 2024.

639 Carpenter, L., Archer, S., and Beale, R.: Ocean-atmosphere trace gas exchange, Chemical Society
640 reviews, 41, 6473-6506, <https://doi.org/10.1039/c2cs35121h>, 2012.

641 Chan, L., and Chan, C.: Role of the Aerosol Phase State in Ammonia/Amines Exchange Reactions,
642 Environmental Science & Technology, 47, 5755-5762, <https://doi.org/10.1021/es4004685>, 2013.

643 Chen, D., Yao, X., Chan, C. K., Tian, X., Chu, Y., Clegg, S. L., Shen, Y., Gao, Y., and Gao, H.:
644 Competitive Uptake of Dimethylamine and Trimethylamine against Ammonia on Acidic Particles
645 in Marine Atmospheres, Environmental Science & Technology, 56, 5430-5439,
646 <https://doi.org/10.1021/acs.est.1c08713>, 2022.

647 Chen, Y., Patel, N., Crombie, A., Scrivens, J., and Murrell, J.: Bacterial flavin-containing
648 monooxygenase is trimethylamine monooxygenase, Proceedings of the National Academy of
649 Sciences, 108, 17791-17796, <https://doi.org/10.1073/pnas.1112928108>, 2011.

650 Chen, Y., Tian, M., Shi, G., Wang, H., Peng, C., Cao, J., Wang, Q., Zhang, S., Guo, D., Zhang, L.,
651 and Yang, F.: Characterization of urban amine-containing particles in southwestern China:
652 Seasonal variation, source, and processing, Atmospheric Chemistry and Physics, 19, 3245-3255,
653 <https://doi.org/10.5194/acp-19-3245-2019>, 2019.

654 Cheng, C., Huang, Z., Chan, C., Chu, Y., Li, M., Zhang, T., Ou, Y., Chen, D., Cheng, P., Lei, L.,
655 Gao, W., Huang, Z., Huang, B., Fu, Z., and Zhou, Z.: Characteristics and mixing state of
656 amine-containing particles at a rural site in the Pearl River Delta, China, Atmospheric Chemistry

657 and Physics, 18, 9147-9159, <https://doi.org/10.5194/acp-18-9147-2018> , 2018.

658 Cheng, G., Hu, Y., Sun, M., Chen, Y., Chen, Y., Zong, C., Chen, J., and Ge, X.: Characteristics and
659 potential source areas of aliphatic amines in PM_{2.5} in Yangzhou, China, Atmospheric Pollution
660 Research, 11, 296-302, <https://doi.org/10.1016/j.apr.2019.11.002> , 2020.

661 Chu, Y., Sauerwein, M., and Chan, C. K.: Hygroscopic and phase transition properties of alkyl
662 aminium sulfates at low relative humidities, Physical Chemistry Chemical Physics, 17,
663 19789-19796, <https://doi.org/10.1039/C5CP02404H> , 2015.

664 Corral, A. F., Choi, Y., Collister, B. L., Crosbie, E., Dadashazar, H., DiGangi, J. P., Diskin, G. S.,
665 Fenn, M., Kirschler, S., Moore, R. H., Nowak, J. B., Shook, M. A., Stahl, C. T., Shingler, T.,
666 Thornhill, K. L., Voigt, C., Ziemba, L. D., and Sorooshian, A.: Dimethylamine in cloud water: a
667 case study over the northwest Atlantic Ocean, Environmental Science: Atmospheres, 2, 1534-1550,
668 <https://doi.org/10.1039/D2EA00117A> , 2022.

669 Dall'osto, M., Airs, R., Beale, R., Cree, C., Fitzsimons, M., Beddows, D., Harrison, R., Ceburnis,
670 D., O'Dowd, C., Rinaldi, M., Paglione, M., Nenes, A., Decesari, S., and Simó, R.: Simultaneous
671 Detection of Alkylamines in the Surface Ocean and Atmosphere of the Antarctic Sympagic
672 Environment, ACS Earth and Space Chemistry, 3, 854-862,
673 <https://doi.org/10.1021/acsearthspacechem.9b00028> , 2019.

674 Du, W., Wang, X., Yang, F., Bai, K., Wu, C., Liu, S., Wang, F., Lv, S., Chen, Y., Wang, J., Liu, W.,
675 Wang, L., Chen, X., and Wang, G.: Particulate Amines in the Background Atmosphere of the
676 Yangtze River Delta, China: Concentration, Size Distribution, and Sources, Advances in
677 Atmospheric Sciences, 38, 1128-1140, <https://doi.org/10.1007/s00376-021-0274-0> , 2021.

678 Facchini, M., Decesari, S., Rinaldi, M., Carbone, C., Finessi, E., Mircea, M., Sandro, F., Moretti,
679 F., Tagliavini, E., Ceburnis, D., and O'Dowd, C.: Important Source of Marine Secondary Organic
680 Aerosol from Biogenic Amines, Environmental Science & Technology, 42, 9116-9121,
681 <https://doi.org/10.1021/es8018385> , 2008a.

682 Facchini, M., Rinaldi, M., Decesari, S., Carbone, C., Finessi, E., Mircea, M., Sandro, F., Ceburnis,
683 D., Flanagan, R., Nilsson, E., de Leeuw, G., Martino, M., Woeltjen, J., and Dowd, C.: Primary
684 submicron marine aerosol dominated by insoluble organic colloids and aggregates, Geophysical
685 Research Letters, 35, L17814, <https://doi.org/10.1029/2008GL034210> , 2008b.

686 Fan, M.-Y., Zhang, Y.-L., Lin, Y.-C., Chang, Y.-H., Cao, F., Zhang, W.-Q., Hu, Y.-B., Bao, M.-Y.,

687 Liu, X.-Y., Zhai, X.-Y., Lin, X., Zhao, Z.-Y., and Song, W.-H.: Isotope-based source
688 apportionment of nitrogen-containing aerosols: A case study in an industrial city in China,
689 Atmospheric Environment, 212, 96-105, <https://doi.org/10.1016/j.atmosenv.2019.05.020> , 2019.

690 Fang, Y., Chen, Y., Tian, C., Lin, T., Hu, L., Li, J., and Zhang, G.: Application of PMF receptor
691 model merging with PAHs signatures for source apportionment of black carbon in the continental
692 shelf surface sediments of the Bohai and Yellow Seas, China, Journal of Geophysical Research:
693 Oceans, 121, 1346-1359, <https://doi.org/10.1002/2015JC011214> , 2016.

694 Feng, H., Ye, X., Liu, Y., Wang, Z., Gao, T., Cheng, A., and Chen, J.: Simultaneous Determination
695 of Nine Atmospheric Amines and Six Inorganic Ions by Non-suppressed Ion Chromatography
696 Using Acetonitrile and 18-Crown-6 as Eluent Additive, Journal of Chromatography A, 461234,
697 <https://doi.org/10.1016/j.chroma.2020.461234> , 2020.

698 Feng, X., Wang, C., Feng, Y., Junjie, C., Zhang, Y., Qi, X., Li, Q., Li, J., and Chen, Y.: Outbreaks
699 of Ethyl-Amines during Haze Episodes in North China Plain: A Potential Source of Amines from
700 Ethanol Gasoline Vehicle Emission, Environmental Science & Technology Letters, 9, 306-311,
701 <https://doi.org/10.1021/acs.estlett.2c00145> , 2022.

702 Gaston, C., Quinn, P., Bates, T., Gilman, J., Bon, D., Kuster, W., and Prather, K.: The impact of
703 shipping, agricultural, and urban emissions on single particle chemistry observed aboard the R/V
704 Atlantis during CalNex, Journal of Geophysical Research: Atmospheres, 118, 5003-5017,
705 <https://doi.org/10.1002/jgrd.50427> , 2013.

706 Ge, X., Wexler, A., and Clegg, S.: Atmospheric amines – Part I. A review, Atmospheric
707 Environment, 45, 524-546, <https://doi.org/10.1016/j.atmosenv.2010.10.012> , 2011a.

708 Ge, X., Wexler, A., and Clegg, S.: Atmospheric amines – Part II. Thermodynamic properties and
709 gas/particle partitioning, Atmospheric Environment, 45, 561-577,
710 <https://doi.org/10.1016/j.atmosenv.2010.10.013> , 2011b.

711 Gibb, S., Mantoura, R., and Liss, P.: Ocean-atmosphere exchange and atmospheric speciation of
712 ammonia and methylamines in the region of the NW Arabian Sea, Global Biogeochemical Cycles,
713 13, 161-178, <https://doi.org/10.1029/98GB00743> , 1999.

714 Gomez-Hernandez, M., McKeown, M., Secrest, J., Marrero-Ortiz, W., Lavi, A., Rudich, Y.,
715 Collins, D. R., and Zhang, R.: Hygroscopic Characteristics of Alkylammonium Carboxylate Aerosols,
716 Environmental Science & Technology, 50, 2292-2300, <https://doi.org/10.1021/acs.est.5b04691> ,

717 2016.

718 Gorzelska, K., and Galloway, J.: Amine nitrogen in the atmospheric environment over the North
719 Atlantic Ocean, *Global Biogeochemical Cycles*, 4, 309-333,
720 <https://doi.org/10.1029/GB004i003p00309> , 1990.

721 Haque, M., Kawamura, K., Deshmukh, D., Cao, F., Song, W., Bao, M., and Zhang, Y.:
722 Characterization of organic aerosols from a Chinese megacity during winter: Predominance of
723 fossil fuel combustion, *Atmospheric Chemistry and Physics*, 19, 5147-5164,
724 <https://doi.org/10.5194/acp-19-5147-2019> , 2019.

725 He, Q., Ding, X., Fu, X.-X., Zhang, Y.-Q., Wang, J.-Q., Liu, Y.-X., Tang, M.-J., Wang, X., and
726 Rudich, Y.: Secondary Organic Aerosol Formation from Isoprene Epoxides in the Pearl River
727 Delta, South China: IEPOX- and HMML-Derived Tracers, *Journal of Geophysical Research:*
728 *Atmospheres*, 123, 6999-7012, <https://doi.org/10.1029/2017JD028242> , 2018.

729 Hemmilä, M., Hellén, H., Virkkula, A., Makkonen, U., Praplan, A., Kontkanen, J., Ahonen, L.,
730 Kulmala, M., and Hakola, H.: Amines in boreal forest air at SMEAR II station in Finland,
731 *Atmospheric Chemistry and Physics*, 18, 6367-6380, <https://doi.org/10.5194/acp-18-6367-2018> ,
732 2018.

733 Hu, Q., Yu, P., Zhu, Y., Li, K., Gao, H., and Yao, X.: Concentration, Size Distribution, and
734 Formation of Trimethylammonium and Dimethylammonium Ions in Atmospheric Particles over
735 Marginal Seas of China, *Journal of the Atmospheric Sciences*, 72, 150522112638006,
736 <https://doi.org/10.1175/JAS-D-14-0393.1> , 2015.

737 Huang, S., Song, Q., Hu, W., Yuan, B., Liu, J., Jiang, B., Li, W., Wu, C., Jiang, F., Chen, W., Wang,
738 X., and Shao, M.: Chemical composition and sources of amines in PM_{2.5} in an urban site of PRD,
739 China, *Environmental Research*, 212, 113261, <https://doi.org/10.1016/j.envres.2022.113261> ,
740 2022.

741 Huang, X., Kao, S.-J., Lin, J., Qin, X., and Deng, C.: Development and validation of a HPLC/FLD
742 method combined with online derivatization for the simple and simultaneous determination of
743 trace amino acids and alkyl amines in continental and marine aerosols, *PLOS ONE*, 13, e0206488,
744 <https://doi.org/10.1371/journal.pone.0206488> , 2018.

745 Johnson, J., and Jen, C.: Role of Methanesulfonic Acid in Sulfuric Acid–Amine and Ammonia
746 New Particle Formation, *ACS Earth and Space Chemistry*, 7, 653-660,

747 <https://doi.org/10.1021/acsearthspacechem.3c00017> , 2023.

748 Kanawade, V. P., and Jokinen, T.: Atmospheric amines are a crucial yet missing link in Earth's
749 climate via airborne aerosol production, *Communications earth & environment*, 6, 98,
750 <https://doi.org/10.1038/s43247-025-02063-0> , 2025.

751 Kang, M., Fu, P., Kawamura, K., Yang, F., Zhang, H., Zang, Z., Ren, H., Ren, L., Zhao, y., Sun, Y.,
752 and Wang, Z.: Characterization of biogenic primary and secondary organic aerosols in the marine
753 atmosphere over the East China Sea, *Atmospheric Chemistry and Physics*, 18, 13947-13967,
754 <https://doi.org/10.5194/acp-18-13947-2018> , 2018.

755 Kleindienst, T., Jaoui, M., Lewandowski, M., Offenberg, J., Lewis, C., Bhave, P., and Edney, E.:
756 Estimates of the contributions of biogenic and anthropogenic hydrocarbons to secondary organic
757 aerosol at a southern US location, *Atmospheric Environment*, 41, 8288-8300,
758 <https://doi.org/10.1016/j.atmosenv.2007.06.045> , 2007.

759 Köllner, F., Schneider, J., Willis, M., Klimach, T., Helleis, F., Bozem, H., Kunkel, D., Hoor, P.,
760 Burkart, J., Leaitch, W. R., Aliabadi, A. A., Abbatt, J., Herber, Andreas, B., and Borrmann, S.:
761 Particulate trimethylamine in the summertime Canadian high Arctic lower troposphere,
762 *Atmospheric Chemistry and Physics*, 17, 13747-13766,
763 <https://doi.org/10.5194/acp-17-13747-2017> , 2017.

764 Lee, D., and Wexler, A.: Atmospheric amines – Part III: Photochemistry and toxicity, *Atmospheric*
765 *Environment*, 71, 95-103, <https://doi.org/10.1016/j.atmosenv.2013.01.058> , 2013.

766 Li, G., Liao, Y., Hu, J., Lu, L., Zhang, Y., Li, B., and An, T.: Activation of NF- κ B pathways
767 mediating the inflammation and pulmonary diseases associated with atmospheric methylamine
768 exposure, *Environmental Pollution*, 252, 1216-1224, <https://doi.org/10.1016/j.envpol.2019.06.059> ,
769 2019a.

770 Li, J., Wang, G., Zhang, q., Li, J., wu, C., Jiang, W., Zhu, T., and Zeng, L.: Molecular
771 characteristics and diurnal variations of organic aerosols at a rural site in the North China Plain
772 with implications for the influence of regional biomass burning, *Atmospheric Chemistry and*
773 *Physics*, 19, 10481-10496, <https://doi.org/10.5194/acp-19-10481-2019> , 2019b.

774 Lidbury, I., Chen, Y., and Murrell, J.: Trimethylamine and trimethylamine N-oxide are
775 supplementary energy sources for a marine heterotrophic bacterium: Implications for marine
776 carbon and nitrogen cycling, *The ISME Journal*, 9, 760-769,

777 <https://doi.org/10.1038/ismej.2014.149> , 2015.

778 Lidbury, I., Mausz, M., Scanlan, D., and Chen, Y.: Identification of dimethylamine
779 monoxygenase in marine bacteria reveals a metabolic bottleneck in the methylated amine
780 degradation pathway, *The ISME Journal*, 11, 1592-1601, <https://doi.org/10.1038/ismej.2017.31> ,
781 2017.

782 Lin, P., Laskin, J., Nizkorodov, S., and Laskin, A.: Revealing Brown Carbon Chromophores
783 Produced in Reactions of Methylglyoxal with Ammonium Sulfate, *Environmental Science &*
784 *Technology*, 49, 14257-14266, <https://doi.org/10.1021/acs.est.5b03608> , 2015.

785 Lin, Q., Zhang, G., Long, P., Bi, X., Wang, X., Brechtel, F., Li, M., Chen, D., Peng, P., and
786 an, Sheng, G., and Zhou, Z.: In situ chemical composition measurement of individual cloud
787 residue particles at a mountain site, southern China, *Atmospheric Chemistry and Physics*, 17,
788 8473-8488, <https://doi.org/10.5194/acp-17-8473-2017> , 2017.

789 Liu, F., Bi, X., Zhang, G., Peng, L., Lian, X., Lu, H., Fu, Y., Wang, X., Peng, P. a., and Sheng, G.:
790 Concentration, size distribution and dry deposition of amines in atmospheric particles of urban
791 Guangzhou, China, *Atmospheric Environment*, 171, 279-288,
792 <https://doi.org/10.1016/j.atmosenv.2017.10.016> , 2017.

793 Liu, F., Bi, X., Zhang, G., Lian, X., Fu, Y., Yang, Y., Lin, Q., Jiang, F., Wang, X., Peng, P. a., and
794 Sheng, G.: Gas-to-particle partitioning of atmospheric amines observed at a mountain site in
795 southern China, *Atmospheric Environment*, 195, 1-11,
796 <https://doi.org/10.1016/j.atmosenv.2018.09.038> , 2018.

797 Liu, T., Xu, Y., Sun, Q., Zhu, R.-G., Li, C. X., Li, Z. Y., Zhang, K. Q., Sun, C. X., and Xiao, H. Y.:
798 Characteristics, Origins, and Atmospheric Processes of Amines in Fine Aerosol Particles in Winter
799 in China, *Journal of Geophysical Research: Atmospheres*, 128, e2023JD038974,
800 <https://doi.org/10.1029/2023JD038974> , 2023.

801 Liu, Z., Li, M., Wang, X., Liang, Y., Jiang, Y., Chen, J., Mu, J., Zhu, Y., Meng, H., Yang, L., Hou,
802 K., Wang, Y., and Xue, L.: Large contributions of anthropogenic sources to amines in fine particles
803 at a coastal area in northern China in winter, *Science of The Total Environment*, 839, 156281,
804 <https://doi.org/10.1016/j.scitotenv.2022.156281> , 2022.

805 Marrero-Ortiz, W., Hu, M., Du, Z., Ji, Y.-M., Wang, Y., Guo, S., Lin, Y., Gomez-Hernandez, M.,
806 Peng, J., Li, Y., Secret, J., Levy Zamora, M., Wang, Y., An, T., and Zhang, R.: Formation and

807 Optical Properties of Brown Carbon from Small α -Dicarbonyls and Amines, Environmental
808 Science & Technology, 53, 117-126, <https://doi.org/10.1021/acs.est.8b03995> , 2018.

809 Medeiros, P., Conte, M., Weber, J., and Simoneit, B.: Sugars as source indicators of biogenic
810 organic carbon in aerosols collected above the Howland Experimental Forest, Maine, Atmospheric
811 Environment, 40, 1694-1705, <https://doi.org/10.1016/j.atmosenv.2005.11.001> , 2006.

812 Milne, P., and Zika, R.: Amino acid nitrogen in atmospheric aerosols: Occurrence, sources and
813 photochemical modification, Journal of Atmospheric Chemistry, 16, 361-398,
814 <https://doi.org/10.1007/BF01032631> , 1993.

815 Miyazaki, Y., Kawamura, K., and Sawano, M.: Size distributions and chemical characterization of
816 water-soluble organic aerosols over the western North Pacific in summer, Journal of Geophysical
817 Research, 115, 210, <https://doi.org/10.1029/2010JD014439> , 2010.

818 Mochida, M., Kawabata, A., Kawamura, K., Hatsushika, H., and Yamazaki, K.: Seasonal variation
819 and origin of dicarboxylic acids in the marine atmosphere over the western North Pacific, Journal
820 of Geophysical Research, 108, 4193, <https://doi.org/10.1029/2002JD002355> , 2003.

821 Müller, C., Iinuma, Y., Karstensen, J., Pinxteren, D., S, L., T, G., and Herrmann, H.: Seasonal
822 variation of aliphatic amines in marine sub-micrometer particles at the Cape Verde Islands,
823 Atmospheric Chemistry and Physics, 9, 9587-9597, <https://doi.org/10.5194/acpd-9-14825-2009> ,
824 2009.

825 Myriokefalitakis, S., Elisabetta, V., Tsigaridis, K., Papadimas, C. D., Sciare, J., Mihalopoulos, N.,
826 Facchini, M., Matteo, R., Dentener, F., Ceburnis, D., Hatzianastassiou, N., O'Dowd, C., van Weele,
827 M., and Kanakidou, M.: Global Modeling of the Oceanic Source of Organic Aerosols, Advances
828 in Meteorology, 2010, 2010, <https://doi.org/10.1155/2010/939171> , 2010.

829 Nakamura, T., Matsumoto, K., and Uematsu, M.: Chemical characteristics of aerosols transported
830 from Asia to the East China Sea: An evaluation of anthropogenic combined nitrogen deposition in
831 autumn, Atmospheric Environment, 39, 1749-1758,
832 <https://doi.org/10.1016/j.atmosenv.2004.11.037> , 2005.

833 Namieśnik, J., Jastrzebska, A., and Zygmunt, B.: Determination of volatile aliphatic amines in air
834 by solid-phase microextraction coupled with gas chromatography with flame ionization detection,
835 Journal of chromatography A, 1016, 1-9, [https://doi.org/10.1016/S0021-9673\(03\)01296-2](https://doi.org/10.1016/S0021-9673(03)01296-2) , 2003.

836 Ng, N., Jimenez, J., Chhabra, P., Seinfeld, J., and Worsnop, D.: Changes in organic aerosol

837 composition with aging inferred from aerosol mass spectra, *Atmospheric Chemistry and Physics*,
838 11, 6465-6474, <https://doi.org/10.5194/acp-11-6465-2011> , 2011.

839 Nielsen, C. J., Herrmann, H., and Weller, C.: Atmospheric chemistry and environmental impact of
840 the use of amines in carbon capture and storage (CCS), *Chemical Society Reviews*, 41, 6684-6704,
841 <https://doi.org/10.1039/c2cs35059a> , 2012.

842 Pankow, J.: Phase Considerations in the Gas/Particle Partitioning of Organic Amines in the
843 Atmosphere, *Atmospheric Environment*, 122, 448-453,
844 <https://doi.org/10.1016/j.atmosenv.2015.09.056> , 2015.

845 Pinxteren, M. V., Fomba, K., Pinxteren, D., Triesch, N., Hoffmann, E., Cree, C., Fitzsimons, M.,
846 Tümping, W., and Herrmann, H.: Aliphatic amines at the Cape Verde Atmospheric Observatory:
847 Abundance, origins and sea-air fluxes, *Atmospheric Environment*, 203, 183-195,
848 <https://doi.org/10.1016/j.atmosenv.2019.02.011> , 2019.

849 Place, B., Quilty, A., Lorenzo, R., Ziegler, S., and VandenBoer, T.: Quantitation of 11 alkyl amines
850 in atmospheric samples: Separating structural isomers by ion chromatography, *Atmospheric*
851 *Measurement Techniques*, 10, 1061-1078, <https://doi.org/10.5194/amt-10-1061-2017> , 2017.

852 Price, D., Clark, C., Tang, X., Cocker, D., Purvis-Roberts, K., and Silva, P.: Proposed chemical
853 mechanisms leading to secondary organic aerosol in the reactions of aliphatic amines with
854 hydroxyl and nitrate radicals, *Atmospheric Environment*, 96, 135-144,
855 <https://doi.org/10.1016/j.atmosenv.2014.07.035> , 2014.

856 Price, D., Kacarab, M., Cocker, D., Purvis-Roberts, K., and Silva, P.: Effects of Temperature on
857 the Formation of Secondary Organic Aerosol from Amine Precursors, *Aerosol Science and*
858 *Technology*, 50, 1216-1226, <https://doi.org/10.1080/02786826.2016.1236182> , 2016.

859 Qiu, C., and Zhang, R.: Multiphase chemistry of atmospheric amines, *Physical Chemistry*
860 *Chemical Physics*, 15, 5738-5752, <https://doi.org/10.1039/c3cp43446j> , 2013.

861 Rinaldi, M., Decesari, S., Finessi, E., Giulianelli, L., Carbone, C., Fuzzi, S., O'Dowd, C. D.,
862 Ceburnis, D., and Facchini, M. C.: Primary and Secondary Organic Marine Aerosol and Oceanic
863 Biological Activity: Recent Results and New Perspectives for Future Studies, *Advances in*
864 *Meteorology*, 2010, 1-10, <https://doi.org/10.1155/2010/310682> , 2010.

865 Rogge, W., Hildemann, L., Mazurek, M., Cass, G., and Simoneit, B.: Sources of Fine Organic
866 Aerosol. 3. Road Dust, Tire Debris, and Organometallic Brake Lining Dust: Roads as Sources and

867 Sinks, Environmental Science & Technology, 27, 1892-1904,
868 <https://doi.org/10.1021/es00046a019> , 1993.

869 Schade, G., and Crutzen, P.: Emission of aliphatic amines from animal husbandry and their
870 reactions: Potential source of N₂O and HCN, Journal of Atmospheric Chemistry, 22, 319-346,
871 <https://doi.org/10.1007/BF00696641> , 1995.

872 Shen, J., Xie, H.-B., Elm, J., ma, F., Chen, J., and Vehkamäki, H.: Methanesulfonic Acid-driven
873 New Particle Formation Enhanced by Monoethanolamine: A Computational Study, Environmental
874 Science & Technology, 53, 14387-14397, <https://doi.org/10.1021/acs.est.9b05306> , 2019.

875 Shen, W., Ren, L., Zhao, Y., Zhou, L., Dai, L., Ge, X., Kong, S., Yan, Q., Xu, H., Jiang, Y., He, J.,
876 Chen, M., and Yu, H.: C1-C2 alkyl aminiums in urban aerosols: Insights from ambient and fuel
877 combustion emission measurements in the Yangtze River Delta region of China, Environmental
878 pollution, 230, 12-21, <https://doi.org/10.1016/j.envpol.2017.06.034> , 2017.

879 Shen, X., Chen, J., and An, T.: A new advance in pollution profile, transformation process, and
880 contribution to SOA formation of atmospheric organic amines, Environmental Science:
881 Atmospheres, 3, 444-473, <https://doi.org/10.1039/D2EA00167E> , 2023.

882 Simoneit, B., Sheng, G., Chen, X., Fu, J., Zhang, J., and Xu, Y.: Molecular marker study of
883 extractable organic matter in aerosols from urban areas of China, Atmospheric Environment Part A
884 General Topics, 25, 2111-2129, [https://doi.org/10.1016/0960-1686\(91\)90088-O](https://doi.org/10.1016/0960-1686(91)90088-O) , 1991.

885 Simoneit, B., Elias, V., Kobayashi, M., Kawamura, K., Rushdi, A., Medeiros, P., Rogge, W., and
886 Didyk, B.: SugarsDominant Water-Soluble Organic Compounds in Soils and Characterization as
887 Tracers in Atmospheric Particulate Matter, Environmental Science & Technology, 38, 5939-5949,
888 <https://doi.org/10.1021/es0403099> , 2004.

889 Sorooshian, A., Murphy, S., Hersey, S., H, G., Padro, L., Nenes, A., Brechtel, F., Jonsson, H.,
890 Flagan, R., and Seinfeld, J.: Comprehensive airborne characterization of aerosol from a major
891 bovine source, Atmospheric Chemistry and Physics, 8, 10415-10479,
892 <https://doi.org/10.5194/acp-8-5489-2008> , 2008.

893 Sun, J., Matusz, M., Chen, Y., and Giovannoni, S.: Microbial Trimethylamine Metabolism in
894 Marine Environments: Microbial TMA metabolism, Environmental Microbiology, 21, 513-520,
895 <https://doi.org/10.1111/1462-2920.14461> , 2019.

896 Tang, X., Price, D., Praske, E., Lee, S. A., Shattuck, M. A., Purvis-Roberts, K., Silva, P. J.,

897 Asa-Awuku, A., and Cocker, D. R.: NO₃ radical, OH radical and O₃-initiated secondary aerosol
898 formation from aliphatic amines, *Atmospheric Environment*, 72, 105-112,
899 <https://doi.org/10.1016/j.atmosenv.2013.02.024> , 2013.

900 Tang, X., Price, D., Praske, E., Vu, D. N., Purvis-Roberts, K., Silva, P. J., Cocker Iii, D. R., and
901 Asa-Awuku, A.: Cloud condensation nuclei (CCN) activity of aliphatic amine secondary aerosol,
902 *Atmospheric Chemistry and Physics*, 14, 5959-5967, <https://doi.org/10.5194/acp-14-5959-2014> ,
903 2014.

904 Van Neste, A., Duce, R. A., and Lee, C.: Methylamines in the Marine Atmosphere, *Geophysical*
905 *Research Letters*, 14, 711-714, <https://doi.org/10.1029/GL014i007p00711> , 1987.

906 VandenBoer, T., Markovic, M., Petroff, A., Czar, M. F., Borduas, N., and Murphy, J. G.: Ion
907 chromatographic separation and quantitation of alkyl methylamines and ethylamines in
908 atmospheric gas and particulate matter using preconcentration and suppressed conductivity
909 detection, *Journal of chromatography A*, 1252, 74-83,
910 <https://doi.org/10.1016/j.chroma.2012.06.062> , 2012.

911 Violaki, K., and Mihalopoulos, N.: Water-soluble organic nitrogen (WSON) in size-segregated
912 atmospheric particles over the Eastern Mediterranean, *Atmospheric Environment*, 44, 4339-4345,
913 <https://doi.org/10.1016/j.atmosenv.2010.07.056> , 2010.

914 Wang, X.-C., and Lee, C.: Sources and distribution of aliphatic amines in salt marsh sediment,
915 *Organic Geochemistry*, 22, 1005-1021, [https://doi.org/10.1016/0146-6380\(94\)90034-5](https://doi.org/10.1016/0146-6380(94)90034-5) , 1994.

916 Welsh, D.: Ecological significance of compatible solute accumulation by micro- organisms: From
917 single cells to global climate, *FEMS Microbiology Reviews*, 24, 263-290,
918 <https://doi.org/10.1111/j.1574-6976.2000.tb00542.x> , 2000.

919 Xie, H., Feng, L., Hu, Q., Zhu, Y., Gao, H., Gao, Y., and Yao, X.: Concentration and size
920 distribution of water-extracted dimethylammonium and trimethylammonium in atmospheric particles
921 during nine campaigns - Implications for sources, phase states and formation pathways, *Science of*
922 *the Total Environment*, 631-632, 130-141, <https://doi.org/10.1016/j.scitotenv.2018.02.303> , 2018.

923 Yang, H., Xu, J., Wu, W.-S., Wan, C., and Yu, J.: Chemical Characterization of Water-Soluble
924 Organic Aerosols at Jeju Island Collected During ACE-Asia, *Environmental Chemistry*, 1, 13-17,
925 <https://doi.org/10.1071/EN04006> , 2004.

926 Yang, X.-Y., Cao, F., Fan, M., Lin, Y. C., Xie, F., and Zhang, Y.: Seasonal variations of low

927 molecular alkyl amines in PM_{2.5} in a North China Plain industrial city: Importance of secondary
928 formation and combustion emissions, *Science of the Total Environment*, 857, 159371,
929 <https://doi.org/10.1016/j.scitotenv.2022.159371> , 2023.

930 Yao, L., Garmash, O., Bianchi, F., Zheng, J., Yan, C., Kontkanen, J., Junninen, H., Mazon, S., Ehn,
931 M., Paasonen, P., Sipilä, M., Wang, M., Wang, X., Xiao, S., Chen, H., Lu, Y., Zhang, B., Wang, D.,
932 Fu, Q., and Wang, L.: Atmospheric new particle formation from sulfuric acid and amines in a
933 Chinese megacity, *Science*, 361, 278-281, <https://doi.org/10.1126/science.aao4839> , 2018.

934 Yin, S., Ge, M.-F., Wang, W., Liu, Z., and Wang, D.: Uptake of gas-phase alkylamines by sulfuric
935 acid, *Chinese Science Bulletin*, 56, 1241-1245, <https://doi.org/10.1007/s11434-010-4331-9> , 2011.

936 You, Kanawade, V., de Gouw, J., Guenther, A., Madronich, S., Sierra-Hernández, M., Lawler, M.,
937 Smith, J., Takahama, S., Ruggeri, G., Koss, A., Olson, K., Baumann, K., Weber, R., Nenes, A.,
938 Guo, H., Edgerton, E., Porcelli, L., Brune, W., and Lee, S.-H.: Atmospheric amines and ammonia
939 measured with a Chemical Ionization Mass Spectrometer (CIMS), *Atmospheric Chemistry and*
940 *Physics*, 14, 12181-12194, <https://doi.org/10.5194/acp-14-12181-2014> , 2014.

941 Yu, P., Hu, Q., Li, K., Zhu, Y., Liu, X., Gao, H., and Yao, X.: Characteristics of dimethylammonium
942 and trimethylammonium in atmospheric particles ranging from supermicron to nanometer sizes over
943 eutrophic marginal seas of China and oligotrophic open oceans, *Science of The Total Environment*,
944 572, 813-824, <https://doi.org/10.1016/j.scitotenv.2016.07.114> , 2016.

945 Zhang, H., Surratt, J., Lin, Y.-H., Bapat, J., and Kamens, R.: Effect of relative humidity on SOA
946 formation from isoprene/NO photooxidation: Enhancement of 2-methylglyceric acid and its
947 corresponding oligoesters under dry conditions, *Atmospheric Chemistry and Physics*, 11,
948 6411-6424, <https://doi.org/10.5194/acp-11-6411-2011> , 2011.

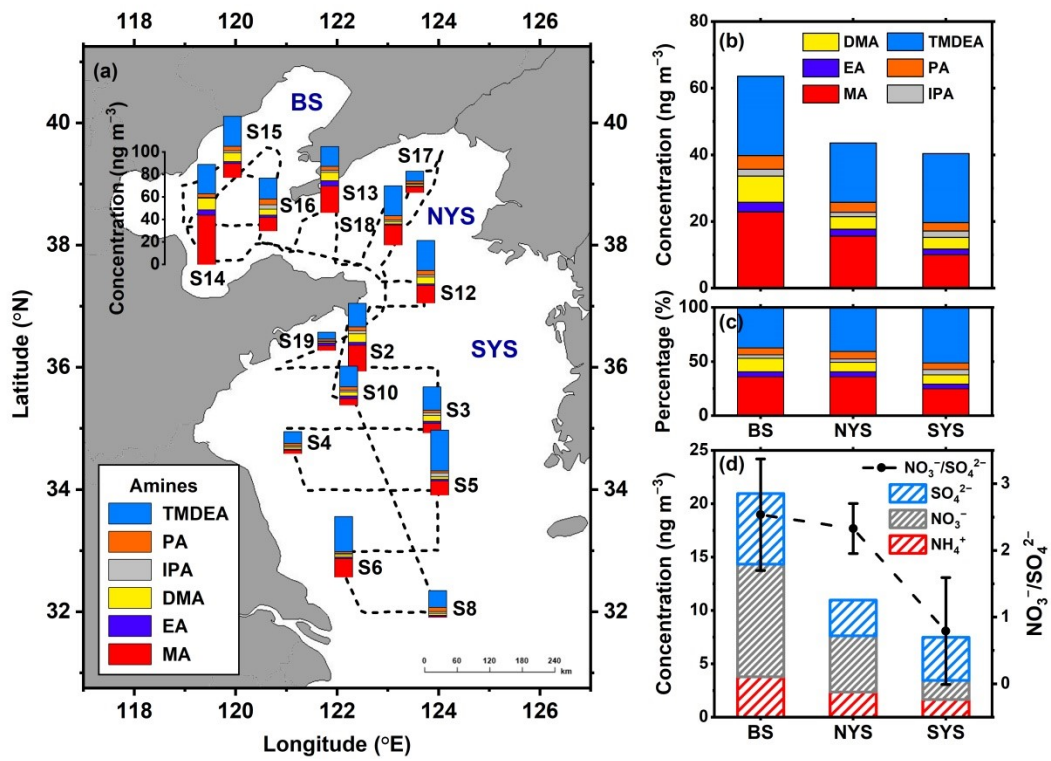
949 Zheng, J., Ma, Y., Chen, M., Zhang, Q., Wang, L., Khalizov, A. F., Yao, L., Wang, Z., Wang, X.,
950 and Chen, L.: Measurement of atmospheric amines and ammonia using the high resolution
951 time-of-flight chemical ionization mass spectrometry, *Atmospheric Environment*, 102, 249-259,
952 <https://doi.org/10.1016/j.atmosenv.2014.12.002> , 2015.

953 Zheng, L., Yang, X., Lai, S., Ren, H., Yue, S., Zhang, Y., Huang, X., Gao, Y., Sun, Y., Wang, Z.,
954 and Fu, P.: Impacts of springtime biomass burning in the northern Southeast Asia on marine
955 organic aerosols over the Gulf of Tonkin, China, *Environmental pollution*, 237, 285-297,
956 <https://doi.org/10.1016/j.envpol.2018.01.089> , 2018.

957 Zhou, S., Li, H., Yang, T., Chen, Y., Deng, C., Gao, Y., Chen, C., and Xu, J.: Characteristics and
958 sources of aerosol aminiums over the eastern coast of China: insights from the integrated
959 observations in a coastal city, adjacent island and surrounding marginal seas, Atmospheric
960 Chemistry and Physics, 19, 10447-10467, <https://doi.org/10.5194/acp-19-10447-2019> , 2019.

961 Zhu, S., Yan, C., Zheng, J., Chen, C., Ning, H., Yang, D., Wang, M., Ma, Y., Zhan, J., Hua, C., Yin,
962 R., Li, Y., Liu, Y., Jiang, J., Yao, L., Wang, L., Kulmala, M., and Worsnop, D.: Observation and
963 Source Apportionment of Atmospheric Alkaline Gases in Urban Beijing, Environmental Science
964 & Technology, 56, 17545-17555, <https://doi.org/10.1021/acs.est.2c03584> , 2022.

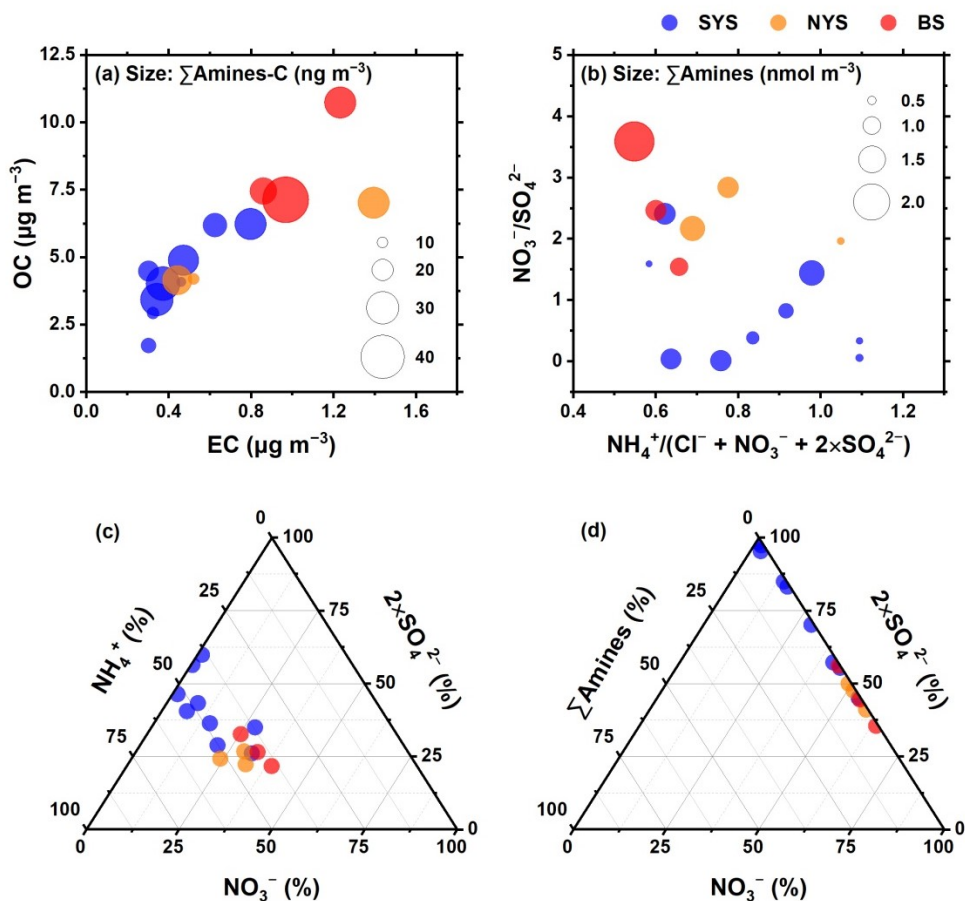
965



966

967 **Figure 1.** Concentrations of amines in 15 TSP samples (a) collected along the cruise
 968 track (black dotted line); average concentrations (b) and relative contributions (c) of
 969 amines; and concentrations of NH₄⁺, NO₃⁻, and SO₄²⁻, along with NO₃⁻/SO₄²⁻ molar
 970 ratios (d), in TSP over the SYS, NYS, and BS.

971



972

973 **Figure 2.** Variations of $\Sigma\text{amines-C}$ with OC and EC concentrations (a); variations of

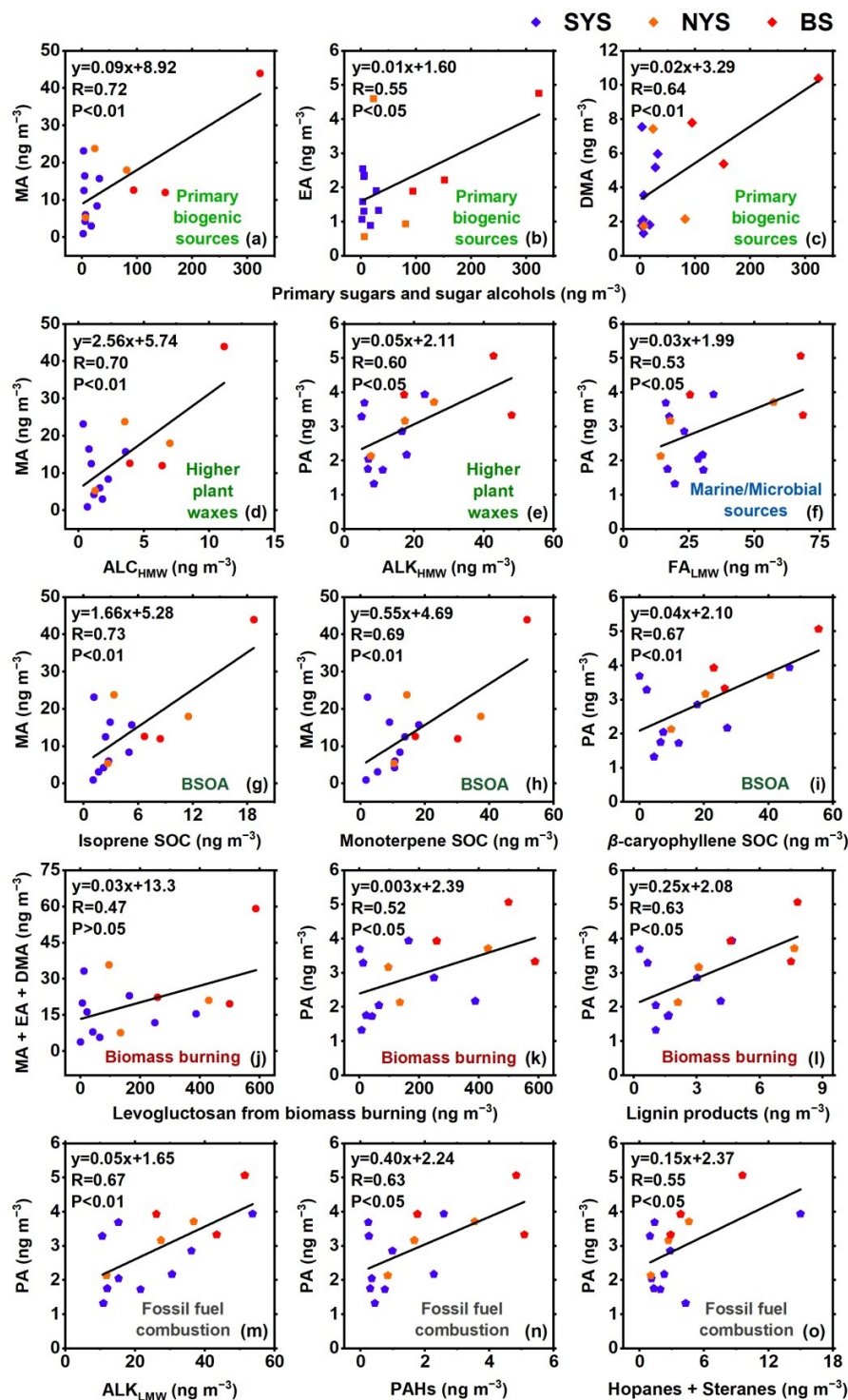
974 Σamines molar concentrations with the $\text{NO}_3^-/\text{SO}_4^{2-}$ and $\text{NH}_4^+ / (\text{Cl}^- + \text{NO}_3^- + 2 \times \text{SO}_4^{2-})$

975 molar ratios (b); ternary diagram of the molar ratio of NH_4^+ , NO_3^- , and SO_4^{2-} (c); and

976 ternary diagram of the molar ratio of Σamines , NO_3^- , and SO_4^{2-} (d) in TSP over the

977 SYS, NYS, and BS.

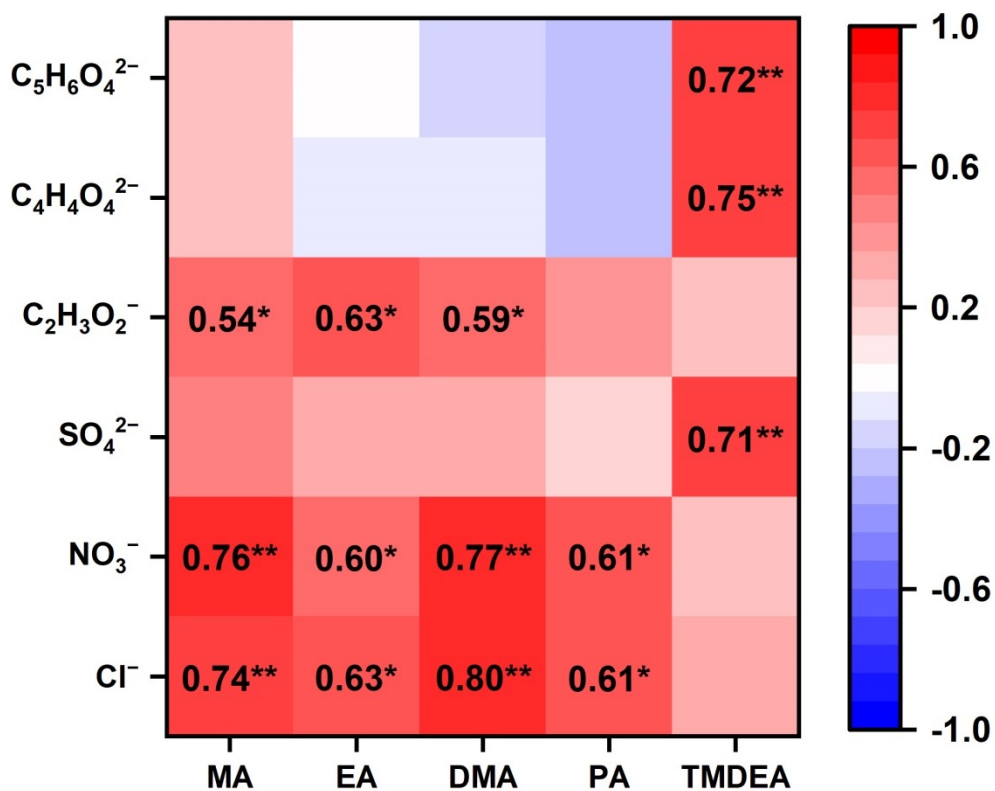
978



979

980 **Figure 3.** Linear regressions between amines and biomarkers (a–i), biomass burning
 981 tracers (j–l), and fossil fuel combustion tracers (m–o) in TSP over the SYS, NYS, and
 982 BS.

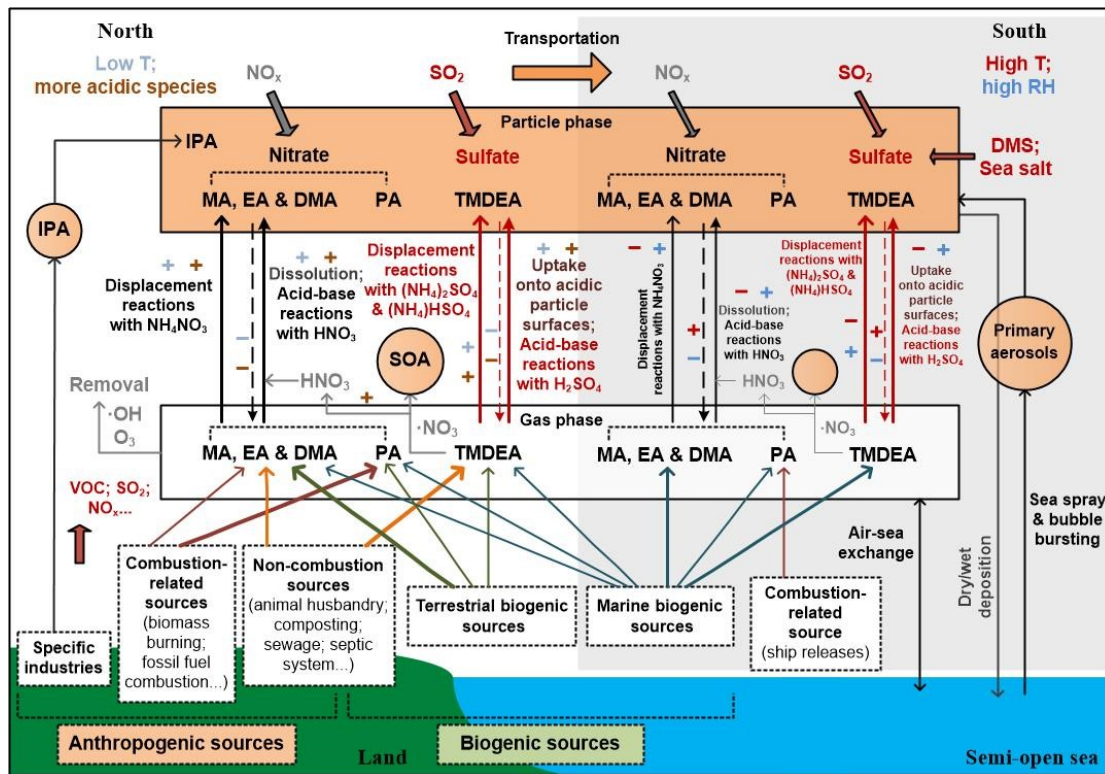
983



984

985 **Figure 4.** Correlation coefficient matrix between amines and acidic species in TSP
 986 over the YS–BS. Numbers indicate correlation coefficients that passed the
 987 significance test; ** denotes $P < 0.01$, and * denotes $P < 0.05$.

988



989

990 **Figure 5.** Schematic diagram illustrating the source contributions and major
 991 secondary formation mechanisms of amines, along with the influences of
 992 environmental conditions over the YS-BS.

993

994